Technical University of Lodz
Faculty of Technical Physics, Information Technology and Applied Mathematics
Institute of Mathematics

Master of Science Thesis

Dynamics of the coupled Hénon maps

by

Patrycja Kuźma

Supervisor: Prof. dr hab. inż. Tomasz Kapitaniak

Łódź, 2012

Contents

Preface

This master of science thesis is a part of "Project TEAM of Foundation for Polish Science" realising the investigation and analysis of the project "Synchronization of Mechanical Systems Coupled through Elastic Structure". It is supported by "Innovative Economy: National Cohesion Strategy". The programme is financed by "Foundation for Polish Science" from the European funds as the plan of "European Regional Development Fund". The project is mainly focused on the following issues:

- Identification of possible synchronous responses of coupled oscillators, and existence of synchronous clusters as well
- Dynamical analysis of identical coupled systems suspended on elastic structure in context of the energy transfer between systems
- Investigation of phase or frequency synchronization effects in groups of coupled non-identical systems
- Developing methods of motion stability control of considered systems
- Investigation of time delay effects in analysed systems
- Developing the idea of energy extraction from ocean waves using a series of rotating pendulums.

INNOVATIVE ECONOMY
NATIONAL COHESION STRATEGY
FNP
Foundation for Polish Science
EUROPEAN UNION
EUROPEAN REGIONAL
DEVELOPMENT FUND

Chapter 1

Introduction

A word synchronization has its origin in ancient Greece and means ’to share the common time’. The studies about synchronization have been the active field of science since 17th century, when Dutch physician Christiaan Huygens performed his experiment concerning two pendulum clocks hanging in the same beam. [1]

In his work *Horologium Oscillatorium* from 1673 Huygens stated: *’It is quite worth noting that when we suspended two clocks so constructed from two hooks imbedded in the same wooden beam, the motions of each pendulum in opposite swings were so much in agreement that they never receded the least bit from each other and the sound of each was always heard simultaneously. Further, if this agreement was disturbed by some interference, it reestablished itself in a short time. For a long time I was amazed at this unexpected result, but after a careful examination finally found that the cause of this is due to the motion of the beam, even though this is hardly perceptible.’*

In this thesis the term synchronization will be understood as a phenomenon, where two or more systems are closely related due to the act of coupling. Systems are coupled if at least one has an effect upon one another. We may distinguish two kinds of coupling: unidirectional and bidirectional. Unidirectional coupling means that one of the coupled system evolves freely and affects the others. Bidirectional coupling refers to systems, which are connected in such a way that they influence each other’s dynamic. The coupling may refer to identical systems as well as to non-identical. [1]

The another point raised here is bistability, which is very common phenomenon in nature. A certain system is said to be bistable if it has two coexisting stable states. We investigate the dynamics of the bidirectionally coupled non-identical bistable Hénon maps. The behaviour of unidirectionally coupled identical bistable Hénon maps has been investigated by J.M. Sausedo-Solorio and A.N. Pisarchik [2].

In following chapters mathematical background, mathematical analysis and results of the numerical research are presented. The thesis is realised within the TEAM programme of Foundation for Polish Science, co-financed from European Union, Regional Development Fund.

1.1 Aim of the thesis

The aim of the thesis is the investigation of the behaviour of the bidirectionally coupled Hénon maps. Firstly, some of the basis properties of the Hénon map will be shown. Next, three bistable maps will be chosen and coupled. Finally, the dynamics of a such coupled system will be analysed.

Chapter 2

Dynamical systems

2.1 Preliminary

Definition 1. *A function* $f : \mathbb{R}^2 \to \mathbb{R}^2$ *is called a* ***map*** *on* $\mathbb{R}^2$.

Let $f : \mathbb{R}^2 \to \mathbb{R}^2$ be a map on $\mathbb{R}^2$.

Definition 2. *The map* f *is called the* ***invertible map*** *if the function* f *is bijection.*

Definition 3. *The map* f *is called the* ***linear map*** *if for every* $(x_1, x_2) \in \mathbb{R}^2$ $f(x_1, x_2) = (a_{11}x_1 + a_{12}x_2, a_{21}x_1 + a_{22}x_2)$, *where* $a_{11}, a_{12}, a_{21}, a_{22} \in \mathbb{R}$ *. [3]*

Definition 4. *Let* $x \in \mathbb{R}^2$*. The set of points* $\{x, f(x), f^2(x), ..\}$ *is called the* ***orbit*** *of* x *under* f*. The point* x*, which starts the orbit, is called the* ***initial value*** *of the orbit. [3]*

Definition 5. *The point* $p \in \mathbb{R}^2$ *is called the* ***fixed point*** *of* f*, when* $f(p) = p$*. [3]*

Definition 6. *The point* $p \in \mathbb{R}^2$ *is called the* ***periodic point of period k*** *if* $f^k(p) = p$ *and* k *is the smallest such positive integer. In this case we say that the orbit with initial value* p *is the* ***periodic orbit of period k****. [3]*

Definition 7. *The* ***phase portrait*** *of* f *is a partitioning of* $\mathbb{R}^2$ *into orbits. [5]*

Definition 8. *A set* $A \subset \mathbb{R}^2$ *is called an* ***invariant set*** *under* f *if for every* $x_0 \in A$ *and for every* $n \in \mathbb{N}$ *we have* $f^n(x_0) \in A$*. [4]*

Definition 9. *We say that a closed invariant set $A \subset \mathbb{R}^2$ is an **attracting set** if there exists some neighbourhood U of the set A such that for every $n \geq 0$ $f^n(U) \subset U$ and $\bigcap_{n>0} f^n(U) = A$.*
*The mentioned set U is called a **trapping region**. [4]*

Remark 1. *If the set A in the definition 9 is a fixed point or a periodic orbit, then we use the term an **attracting fixed point** or an **attracting periodic orbit**.*

Definition 10. *Let $A \subset \mathbb{R}^2$ be an attracting set and $U \subset \mathbb{R}^2$ any trapping region of A. A set $\bigcup_{n\geq 0} f^{-n}(U)$ is called **basin of attraction** of a set A. [4]*

Remark 2. *$f^{-1}(U)$ in definition 10 is understood as the preimage of the set U, so for every $n > 0$ $f^{-n}(U)$ makes sense even if a map f is not invertible.*

Definition 11. *A closed invariant set $A \subset \mathbb{R}^2$ is topologically transitive if for every two open sets $U, V \subset A$, there exists $n > 0$ such that $f^n(U) \cap V \neq \emptyset$. [4]*

Definition 12. *An **attractor** is a topologically transitive attracting set. [4]*

Definition 13. *We say that f has **sensitive dependence on initial conditions** on $A \subset \mathbb{R}^2$ if there exists $\varepsilon > 0$ such that, for every $x \in A$ and every neighbourhood U of x, there exists $y \in U$ and there exists $n > 0$ such that $|f^n(x) - f^n(y)| > \varepsilon$. [4]*

Definition 14. *A set $A \subset \mathbb{R}^2$ is called **chaotic** if:*

- *f has sensitive dependence on initial value on set A;*
- *f is topologically transitive on set A;*
- *the periodic orbits of f are dense in set A. [4]*

Definition 15. *Let $A \subset \mathbb{R}^2$ be an attractor. If set A is chaotic, it is called a **strange attractor**. [4]*

2.2 Analyses of fixed points and period orbits

Definition 16. *Let $p \in \mathbb{R}^2$ and let $f = (f_1, f_2)$ be a C^1 map on $\mathbb{R}^2$. The matrix*

$$\boldsymbol{Df}(x) := \begin{pmatrix} \dfrac{\partial f_1}{\partial x_1}(x) & \dfrac{\partial f_1}{\partial x_2}(x) \\ \dfrac{\partial f_2}{\partial x_1}(x) & \dfrac{\partial f_2}{\partial x_2}(x) \end{pmatrix}$$

is called the ***Jacobian matrix*** *of map f at point x. [3]*

Definition 17. *Let A be a square matrix and let $\mathbb{I}$ be identity matrix. The solutions λ of equation $\det(A - \lambda\mathbb{I}) = 0$ are called the* ***eigenvalues*** *of matrix A. [3]*

Theorem 1. *Let $p \in \mathbb{R}^2$ be a fixed point of f and let $\lambda_{1,2}$ be the eigenvalues of $\boldsymbol{Df}(p)$.*

- *If $|\lambda_1| < 1$ and $|\lambda_2| < 1$, then the point p is the attracting fixed point.*
- *If $|\lambda_1| > 1$ and $|\lambda_2| > 1$, then the point p is not the attracting fixed point.*
- *If $|\lambda_1| > 1$ and $|\lambda_2| < 1$, then the point p is not the attracting fixed point. [3]*

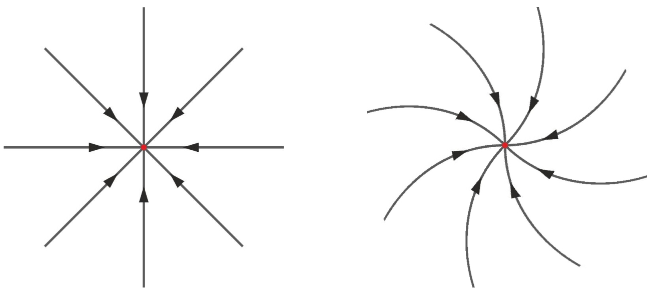

Figure 1. *The behaviour of orbits in the neighbourhoods of exemplary attracting fixed points.*

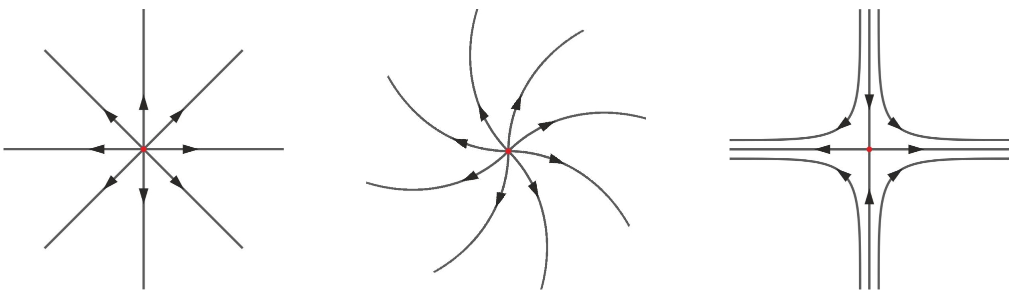

Figure 2. *The behaviour of orbits in the neighbourhoods of exemplary fixed points, which are not attracting.*

Theorem 2. *Let $\{p_1, ..., p_k\}$, where for $i \in \{1, ..., k\}$ $p_i \in \mathbb{R}^2$, be a periodic orbit of period k of the map f and let λ_1, λ_2 be the eigenvalues of $\boldsymbol{Df}^{\,k}(p_1)$.*

- *If $|\lambda_1| < 1$ and $|\lambda_2| < 1$, then $\{p_1, ..., p_k\}$ is the attracting periodic orbit.*
- *If $|\lambda_1| > 1$ and $|\lambda_2| > 1$, then $\{p_1, ..., p_k\}$ is not the attracting periodic orbit.*
- *If $|\lambda_1| > 1$ and $|\lambda_2| < 1$, then $\{p_1, ..., p_k\}$ is not the attracting periodic orbit.[3]*

Remark 3. *While using the theorem 2 and computing $\boldsymbol{Df}^k(p_1)$ the equality*

$$\boldsymbol{Df}^k(p_1) = \boldsymbol{Df}(p_k) \cdot \boldsymbol{Df}(p_{k-1}) \cdot ... \cdot \boldsymbol{Df}(p_1)$$

might be helpful. [3]

2.3 Bifurcations

The term 'bifurcation' means the sudden change of dynamics of the map (for example its set of fixed points and period orbits) as some parameter is varied. There exist a range of possible bifurcations, but we will focus on so called period-doubling bifurcation.

In this section we will consider a r-parameter family of maps on $\mathbb{R}^n$:

$$g(x, p) = (g_1(x, p), g_2(x, p), ..., g_n(x, p)), \quad x \in \mathbb{R}^n, \quad p \in \mathbb{R}^r,$$

where x is variable, p is parameter and $g : \mathbb{R}^n \times \mathbb{R}^r \to \mathbb{R}^n$ is C^1 function.

Definition 18. *Let λ_1 be the eigenvalue of the matrix* $\begin{pmatrix} \frac{\partial g_1}{\partial x_1}(x,p) & ... & \frac{\partial g_1}{\partial x_n}(x,p) \\ \vdots & & \vdots \\ \frac{\partial g_n}{\partial x_1}(x,p) & ... & \frac{\partial g_n}{\partial x_n}(x,p) \end{pmatrix}$. *The bifurcation associated with the appearance of $\lambda_1 = -1$ is called a **flip** or **period-doubling** bifurcation. [5]*

Period doubling bifurcation is connected with emerging of new period $2k$ orbit from period k orbit, where $k \in \mathbb{N}$.

Remark 4. *The appearance of $\lambda_1 = -1$ is only a necessary condition for existing a period doubling bifurcation.*

Definition 19. *A **bifurcation diagram** is a stratification of parameters together with representative orbits (or its projections) for each stratum. [5]*

Now, we will analyse the example presented by Yuri A. Kuznetsov in [5]. The example concerns one-dimensional map with one parameter.

Example 1. *Let us define:*

$$f(x,a) \equiv f_a(x) = -(1+a)x + x^3, \tag{2.1}$$

where $x \in \mathbb{R}$ is variable and $a \in \mathbb{R}$ is parameter.
For the one-dimensional map g a fixed point x_0 is attracting if $|g'_x(x_0)| < 1$ and it not attracting if $|g'_x(x_0)| > 1$. $g'_x(x_0)$ is an equivalent of the eigenvalue for one-dimensional map.
It is easy to notice that $x = 0$ is a fixed point of (2.1). We will analyse (2.1) only in the neighbourhood of $x = 0$. For the analysed map (2.1) $f'_x(x,a) = -(1-a) + 3x^2$, hence $|f'_x(0,a)| = |1-a|$. We have that $|f'_x(0,a)| < 1$, then $a \in (0,2)$ and $|f'_x(0,a)| > 1$, then $a \in (-\infty,0) \cup (2,\infty)$. Therefore we may say that $x = 0$ is attracting fixed point for sufficiently small $a > 0$ and it is not attracting fixed point for sufficiently small $a < 0$. What is more $f'_x(0,0) = -1$, what is a necessary condition for existing a period doubling bifurcation. Considering bifurcation diagram presented in figure 3 we may be sure that for $a = 0$ a period-doubling bifurcation occurs.

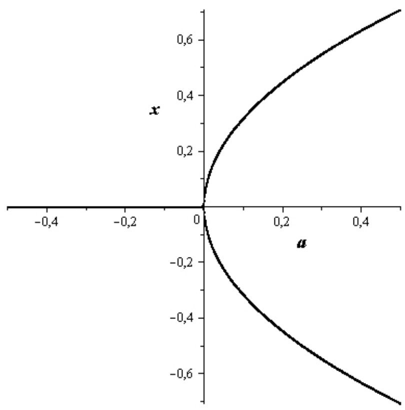

Figure 3. *Bifurcation diagram for map (2.1).*

Example 2. *The most popular map, where period-doubling occurs is the logistic map:*

$$f(x,a) \equiv ax(1-x), \tag{2.2}$$

where $x \in [0,1]$ is variable and $a \in [1,4]$ is parameter.

We will analyse the following bifurcation diagram created for the map (2.2):

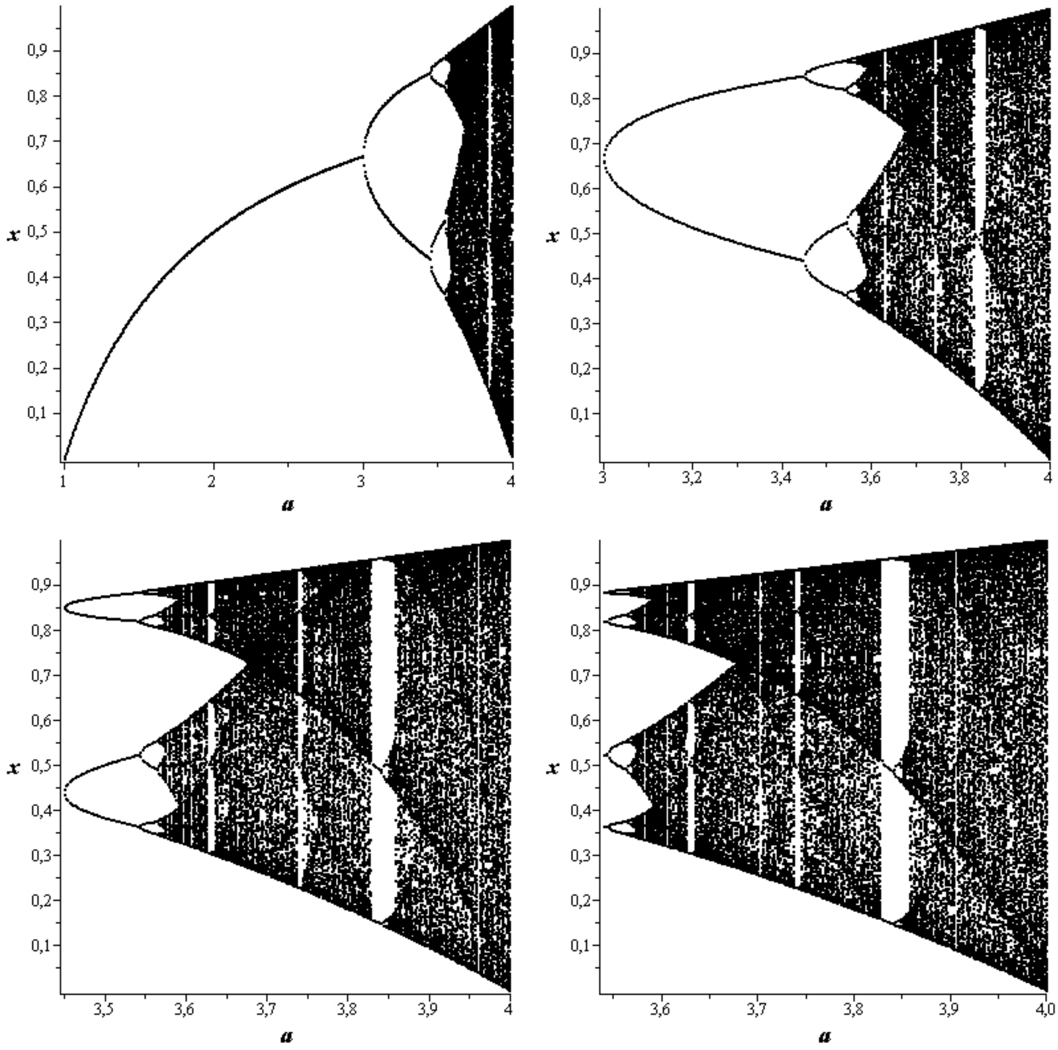

Figure 4. *Bifurcation diagram for map (2.2) for $a \in [1,4]$ and its enlarged views.*

As might be seen in figure 4 for $a \in [1,3]$ there exists attracting fixed point, which bifurcates via period doubling into period 2 orbit at $a = 3$. The mentioned attracting period 2 orbit stops being attracting and attracting period 4 orbit emerge at $a = 3.45$. Increasing parameter a further period-doubling occurs till the emerging of chaotic attractor.

Chapter 3

The Hénon map

A map proposed by French mathematician and astronomer Michel Hénon is a simple two-dimensional model with a complicated dynamic.
Michel Hénon presented a following map:

$$H(x, y) \equiv (1 - ax^2 + y, -bx),$$

where a and b are real parameters.
The model $H(x, y)$ is known as **the Hénon map**.
$H(x, y)$ is the composition of the following transformations of the point $(x, y) \in \mathbb{R}^2$:

- $H'(x, y) = (x, 1 + y - ax^2)$, where a is real parameter (H' simulate the folding);
- $H''(x, y) = (-bx, y)$, where b is real parameter (H'' contracts or enlarge area along the x-axis);
- $H'''(x, y) = (y, x)$ (H''' changes the orientation). [6]

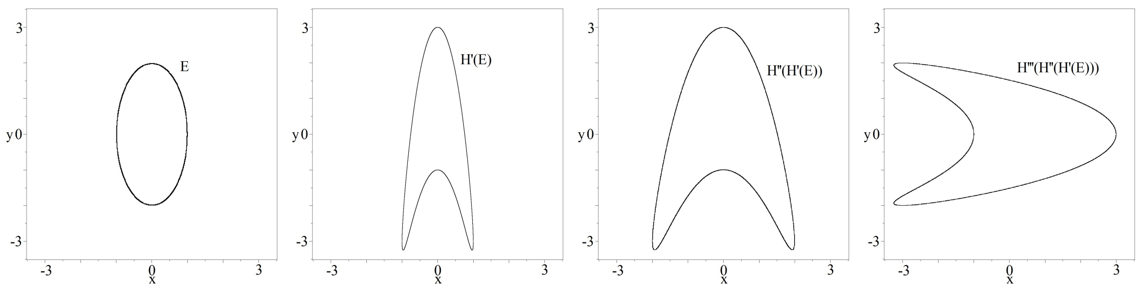

Figure 5. *Transformations H', $H'' \circ H'$ and $H''' \circ H'' \circ H'$ of the ellipse $E = \left\{(x, y) \in \mathbb{R}^2 : x^2 + \left(\frac{y}{2}\right)^2 = 1\right\}$ for $a = 4$ and $b = -2$.*

Theorem 3. *A map $H(x, y)$, where $b \neq 0$, is invertible.*

Proof. Firstly, we will show that $H(x, y)$ is a surjective function. Let $(u, v) \in \mathbb{R}^2$. We will show that there exists $(x, y) \in \mathbb{R}^2$ such that $H(x, y) = (u, v)$. To find such $(x, y) \in \mathbb{R}^2$, we consider system of equations given by:

$$\begin{cases} 1 - ax^2 + y = u \\ -bx = v \end{cases}$$

Assuming $b \neq 0$, we obtain from the second equation $x = -\frac{v}{b}$. Substituting it into the first one we receive:

$$1 - a\left(\frac{v}{b}\right)^2 + y = u$$

This way we obtain that $y = u - 1 + a\left(\frac{v}{b}\right)^2$.
In conclusion we found $(x, y) = (-\frac{v}{b}, u-1+a\left(\frac{v}{b}\right)^2)$ such that $H(x, y) = (u, v)$ unless $b = 0$. According to definition 1, we proved $H(x, y)$ is a map on $\mathbb{R}^2$ unless $b = 0$. Let us observe what happens if $b = 0$. If $b = 0$, then $H(x, y)$ takes the form $H(x, y) = (1 - ax^2 + y, 0)$. It may be easily noticed that $H(x, y)$ is not a surjective function. For example let $(u, v) = (0, 1) \in \mathbb{R}^2$. Let us assume that there exists $(x, y) \in \mathbb{R}^2$ such that $H(x, y) = (0, 1)$. Hence we get:

$$\begin{cases} 1 - ax^2 + y = 0 \\ 0 = 1 \end{cases}$$

What leads us automatically to contradiction. Therefore we obtain that $H(x, y)$ is not surjective function for $b = 0$ and in consequence $H(x, y)$ is not an invertible map on $\mathbb{R}^2$ for $b = 0$.

Now, we will show that $H(x, y)$ is a injective function. Let $(x, y), (\tilde{x}, \tilde{y}) \in \mathbb{R}^2$ and let $b \neq 0$. To prove that a map H is injective function, we have to show that if $H(x, y) = H(\tilde{x}, \tilde{y})$, then $(x, y) = (\tilde{x}, \tilde{y})$. Hence let us assume that $H(x, y) = H(\tilde{x}, \tilde{y})$, what is equivalent to:

$$\begin{cases} 1 - ax^2 + y = 1 - a\tilde{x}^2 + \tilde{y} \\ -bx = -b\tilde{x} \end{cases}$$

From the second equation we immediately obtain that $x = \tilde{x}$. Substituting it into the first equation we obtain: $1-ax^2+y = 1-ax^2+\tilde{y}$. Hence $y = \tilde{y}$. In a consequence we have that $(x, y) = (\tilde{x}, \tilde{y})$.
Now we will show that $H^{-1}(x, y) = (-\frac{y}{b}, x - 1 + a\left(\frac{y}{b}\right)^2)$ is the inverse of $H(x, y)$. Considering $H(H^{-1}(x, y))$ and $H^{-1}(H(x, y))$ we have:
$H(H^{-1}(x, y)) = H\left(-\frac{y}{b}, x - 1 + a\left(\frac{y}{b}\right)^2\right) = \left(1 - a\left(\frac{-y}{b}\right)^2 + x - 1 + a\left(\frac{y}{b}\right)^2, -b\frac{-y}{b}\right) =$ (x, y) and $H^{-1}(H(x, y)) = H^{-1}(1-ax^2+y, -bx) = \left(-b\frac{-x}{b}, 1 - ax^2 + y - 1 + a\left(\frac{-bx}{b}\right)^2\right) =$ (x, y)
Hence H^{-1} is indeed the inverse of $H(x, y)$.

□

3.1 Area-contraction

Firstly, we will find the condition, which parameters in $H(x, y)$ must fulfil to enable the occurring of attracting sets. In this purpose the following definitions and theorems will be introduced:

Definition 20. *A map $f : \mathbb{R}^2 \to \mathbb{R}^2$ is called **area-contracting**, if for every non-empty Borel set $B \subset \mathbb{R}^2$, the area of $f(B)$ is less than the area of B. [8]*

Definition 21. *A map $f : \mathbb{R}^2 \to \mathbb{R}^2$ is called **area-preserving**, if for every non-empty Borel set $B \subset \mathbb{R}^2$, the area of $f(B)$ is equal to the area of B.*

Definition 22. *A map $f : \mathbb{R}^2 \to \mathbb{R}^2$ is called **area-expanding**, if for every non-empty Borel set $B \subset \mathbb{R}^2$, the area of $f(B)$ is greater then the area of B.*

Lemma 1. *Let Δ and D be Borel sets in $\mathbb{R}^2$. Assume that $f : \Delta \to D$ is a bijection and has continuous partial derivatives in Δ. If $g : D \to \mathbb{R}$ is a continuous function, then:*

$$\iint\limits_{D} g(y)dy_1dy_2 = \iint\limits_{\Delta} g(f(x))|\det \boldsymbol{Df}(x)|dx_1dx_2. \text{ [7]}$$

Theorem 4. *Let f be invertible C^1 map on $\mathbb{R}^2$.*

- *If for every $x \in \mathbb{R}^2$ $|\det \boldsymbol{Df}(x)| < 1$, then the map f is area-contracting.*
- *If for every $x \in \mathbb{R}^2$ $|\det \boldsymbol{Df}(x)| = 1$, then the map f is area-preserving.*
- *If for every $x \in \mathbb{R}^2$ $|\det \boldsymbol{Df}(x)| > 1$, then the map f is area-expanding. [3]*

Proof. Let f be invertible C^1 map on $\mathbb{R}^2$ and let B be a Borel set.
Firstly, let us assume that for every $x = (x_1, x_2) \in \mathbb{R}^2$ $|\det \mathbf{Df}(x)| < 1$. Using the lemma 1 (with $\Delta = B$ and with $g(y) = 1$ for every $y \in f(B)$) and by the assumption we have:

$$|f(B)| = \iint\limits_{f(B)} 1 dy_1 dy_2 = \iint\limits_{B} |\det \mathbf{Df}(x)| dx_1 dx_2 < \iint\limits_{B} 1 dx_1 dx_2 = |B|$$

Hence the map f is area-contracting.
Now, let us assume that for every $x = (x_1, x_2) \in \mathbb{R}^2$ $|\det \mathbf{Df}(x)| = 1$. By analogy we obtain:

$$|f(B)| = \iint\limits_{f(B)} 1 dy_1 dy_2 = \iint\limits_{B} |\det \mathbf{Df}(x)| dx_1 dx_2 = \iint\limits_{B} 1 dx_1 dx_2 = |B|$$

That proves that map f is area-preserving.
Assuming that for every $x = (x_1, x_2) \in \mathbb{R}^2$ $|\det \mathbf{Df}(x)| > 1$, analogously we have:

$$|f(B)| = \iint\limits_{f(B)} 1 dy_1 dy_2 = \iint\limits_{B} |\det \mathbf{Df}(x)| dx_1 dx_2 > \iint\limits_{B} 1 dx_1 dx_2 = |B|$$

Hence the map f is area-expanding.

$\square$

Theorem 5. *For every $(x,y) \in \mathbb{R}^2$ the absolute value of the determinant of $\boldsymbol{DH}(x,y)$ is equal to $|b|$. Moreover:*

- *If $|b| < 1$, then the Hénon map $H(x,y)$ is area-contracting.*
- *If $|b| = 1$, then the Hénon map $H(x,y)$ is area-preserving.*
- *If $|b| > 1$, then the Hénon map $H(x,y)$ is area-expanding.*

Proof. Let $(x,y) \in \mathbb{R}^2$ and let $H(x,y) = (H_1(x,y), H_2(x,y)) = (1 - ax^2 + y, -bx)$. Computing

$$|\det \mathbf{DH}(x,y)| = \left|\det \begin{pmatrix} \frac{\partial H_1}{\partial x}(x,y) & \frac{\partial H_1}{\partial y}(x,y) \\ \frac{\partial H_2}{\partial x}(x,y) & \frac{\partial H_2}{\partial y}(x,y) \end{pmatrix}\right| = \left|\det \begin{pmatrix} -2ax & 1 \\ -b & 0 \end{pmatrix}\right| = |b|,$$

by theorem 4 we obtain that for $|b| < 1$ $H(x,y)$ is area-contracting, for $|b| = 1$ $H(x,y)$ is area-preserving and $|b| > 1$ $H(x,y)$ is area-expanding.

□

Theorem 6. *If the Hénon map $H(x,y)$ has an attracting set, then $|b| < 1$.*

Proof. We assume that $H(x,y)$ has an attracting set $A \subset \mathbb{R}^2$ and that, to the contrary, $|b| \geq 1$. We will consider two cases: $|b| > 1$ and $|b| = 1$.

Let $|b| > 1$. As $H(x,y)$ has an attracting set $A \subset \mathbb{R}^2$, let $U \subset \mathbb{R}^2$ be a trapping region of A. By definition 9, a trapping region fulfils $H(U) \subset U$. That leads to the conclusion that the area of $H(U)$ is less or equal to the area of U. On the other hand, by theorem 5 $H(x,y)$ is area-expanding, so the area of $H(U)$ is greater than area of U. Hence, we obtain a contradiction.

Let $|b| = 1$. Hence by theorem 5 $H(x,y)$ is area-preserving. According to definition 9, there exists a neighbourhood U of the set A such that for every $n \geq 0$ $H^n(U) \subset U$ and $\bigcap_{n>0} H^n(U) = A$. As for every $n \geq 0$ $H^n(U) \subset U$ and the area of $H(U)$ is equal to the area of U, we have that for every $n \geq 0$ $H^n(U) = U$. Therefore we have that $\bigcap_{n>0} H^n(U) = U$, but $U \neq A$ as U is a neighbourhood of A. This way we get a contradiction.

□

3.2 Bifurcations

Now, we will analyse the behaviour of the $H(x, y)$ connected with emerging of fixed points and period orbits.

Remark 5. *If $a = 0$, then $H(x, y)$ is a trivial linear map.*

Theorem 7. *Let us assume that $a \neq 0$.*

- *If $(b+1)^2 + 4a < 0$, then $H(x, y)$ does not have fixed points.*
- *If $(b+1)^2 + 4a = 0$, then $H(x, y)$ has one fixed point:* $(x, y) = \left(\frac{-(b+1)}{2a}, \frac{b(b+1)}{2a}\right)$.
- *If $(b+1)^2 + 4a > 0$, then $H(x, y)$ has two fixed points:* $(x, y) = \left(\frac{-(b+1)+\sqrt{(b+1)^2+4a}}{2a}, b\frac{(b+1)-\sqrt{(b+1)^2+4a}}{2a}\right)$, $(x, y) = \left(\frac{-(b+1)-\sqrt{(b+1)^2+4a}}{2a}, b\frac{(b+1)+\sqrt{(b+1)^2+4a}}{2a}\right)$.

Proof. Let $a \neq 0$. In order to find fixed points of $H(x, y)$, we consider equation $H(x, y) = (x, y)$. Hence we have:

$$\begin{cases} x = 1 - ax^2 + y \\ y = -bx, \end{cases}$$

what implies:

$$ax^2 + (1+b)x - 1 = 0. \tag{3.1}$$

Due to the fact $\Delta_1 = (1+b)^2 + 4a$, we have:
For $\Delta_1 < 0$ $H(x, y)$ does not have fixed points.
For $\Delta_1 = 0$ $H(x, y)$ has one fixed point: $(x, y) = \left(\frac{-(b+1)}{2a}, \frac{b(b+1)}{2a}\right)$.
For $\Delta_1 > 0$ $H(x, y)$ has two fixed points:

$$(x, y) = \left(\frac{-(b+1)+\sqrt{(b+1)^2+4a}}{2a}, b\frac{(b+1)-\sqrt{(b+1)^2+4a}}{2a}\right),$$

$$(x, y) = \left(\frac{-(b+1)-\sqrt{(b+1)^2+4a}}{2a}, b\frac{(b+1)+\sqrt{(b+1)^2+4a}}{2a}\right).$$

□

Theorem 8. *The eigenvalues of the Jacobian matrix of the Hénon map $H(x,y)$ are: $\lambda_1 = -ax - \sqrt{a^2x^2 - b}$ and $\lambda_2 = -ax + \sqrt{a^2x^2 - b}$. Furthermore, the following relations are fulfilled: $\lambda_1 + \lambda_2 = -2ax$ and $\lambda_1\lambda_2 = b$.*

Proof. Let $(x,y) \in \mathbb{R}^2$ and let $H(x,y) = (H_1(x,y), H_2(x,y)) = (1 - ax^2 + y, -bx)$. To obtain the eigenvalues of $\mathbf{DH}(x,y)$ we are searching for the roots of function $\det(\mathbf{DH}(x,y) - \lambda\mathbb{I})$:

$$\det(\mathbf{DH}(x,y) - \lambda\mathbb{I}) = \det \begin{pmatrix} \frac{\partial H_1}{\partial x}(x,y) - \lambda & \frac{\partial H_1}{\partial y}(x,y) \\ \frac{\partial H_2}{\partial x}(x,y) & \frac{\partial H_2}{\partial y}(x,y) - \lambda \end{pmatrix} =$$

$$= \det \begin{pmatrix} -2ax - \lambda & 1 \\ -b & -\lambda \end{pmatrix} = \lambda(2ax + \lambda) + b = \lambda^2 + 2ax\lambda + b = 0$$

Hence we get two eigenvalues of $\mathbf{DH}(x,y)$ $\lambda_1 = -ax - \sqrt{a^2x^2 - b}$ and $\lambda_2 = -ax + \sqrt{a^2x^2 - b}$. Moreover, using the Vieta's formulas we get that: $\lambda_1 + \lambda_2 = -2ax$ and $\lambda_1\lambda_2 = b$.

□

Theorem 9. *Let $a \neq 0$.*
If period doubling bifurcation connected with emerging of period 2 orbit occurs for $H(x,y)$, then it takes place for parameters fulfilling the relation $a = \frac{3}{4}(1+b)^2$

Proof. Let λ_1, λ_2 be the eigenvalues of $\mathbf{DH}(x,y)$. Assuming that $\lambda_1 = -1$ and using the theorem 8 we easily obtain the relation:

$$b + 1 = 2ax. \tag{3.2}$$

According to theorem 7 if (x,y) is a fixed point, then

$$x = \frac{-(b+1) \pm \sqrt{(b+1)^2 + 4a}}{2a}. \tag{3.3}$$

Now putting (3.3) into (3.2) we have that

$$2(b+1) = \pm\sqrt{(b+1)^2 + 4a}$$

what after considering two cases ($b \geq -1$ and $b < -1$) implies that $a = \frac{3}{4}(b+1)^2$.

□

Theorem 10. *Let us assume that* $a \neq 0$.
$H(x,y)$ has period orbit of period 2 if and only if $4a > 3(b+1)^2$.
Moreover, that period orbit consist of: $(x,y) = \left(\frac{(b+1)+\sqrt{4a-3(b+1)^2}}{2a}, -b\frac{(b+1)-\sqrt{4a-3(b+1)^2}}{2a}\right)$ *and* $(x,y) = \left(\frac{(b+1)-\sqrt{4a-3(b+1)^2}}{2a}, -b\frac{(b+1)+\sqrt{4a-3(b+1)^2}}{2a}\right)$.

Proof. Let $a \neq 0$. In order to find periodic point of period two of $H(x,y)$, we consider equation $H^2(x,y) = (x,y)$, what is equivalent to:

$$\begin{cases} x = 1 - a(1 - ax^2 + y)^2 - bx \\ y = -b(1 - ax^2 + y), \end{cases} \tag{3.4}$$

Assuming that $b \neq -1$, we solve the second equation for y and substitute into the first, obtaining:

$$(ax^2 + (b+1)x - 1)(a^2x^2 - (b+1)ax - a + (b+1)^2) = 0 \tag{3.5}$$

Firstly we will focus on the left factor of equation (3.5)

$$ax^2 + (b+1)x - 1 = 0, \tag{3.6}$$

which is the same as the equation (3.1).
The solutions of (3.6) are $x = \frac{-(b+1)\pm\sqrt{(b+1)^2+4a}}{2a}$ if $(b+1)^2 + 4a \geq 0$ and (3.6) has no solutions for $(b+1)^2 + 4a < 0$. Substituting those points into the second equation in (3.4) we obtain the following solution for $(b+1)^2 + 4a \geq 0$:
$\left(\frac{-(b+1)+\sqrt{(b+1)^2+4a}}{2a}, b\frac{(b+1)-\sqrt{(b+1)^2+4a}}{2a}\right)$ and $\left(\frac{-(b+1)-\sqrt{(b+1)^2+4a}}{2a}, b\frac{(b+1)+\sqrt{(b+1)^2+4a}}{2a}\right)$.
According to theorem 7 those points are the fixed points of $H(x,y)$. That result is a consequence of the fact that fixed points of $H(x,y)$ are also fixed points of $H^2(x,y)$. Hence to find periodic point of period two, we consider equation:

$$ax^2 - (b+1)x + \frac{-a + (b+1)^2}{a} = 0 \tag{3.7}$$

Let us notice that determinant of equation (3.7) is equal to $\Delta_2 = -3(b+1)^2 + 4a$. As a result $H(x,y)$ has a period-two orbit, if $\Delta_2 > 0$, what is equivalent to $4a > 3(b+1)^2$. Solving (3.7) and substituting the result into the second equation in (3.5) we obtain that considered period 2 orbit consist of the following points:

$$(x,y) = \left(\frac{(b+1)+\sqrt{4a-3(b+1)^2}}{2a}, -b\frac{(b+1)-\sqrt{4a-3(b+1)^2}}{2a}\right)$$

and

$$(x,y)=\left(\frac{(b+1)-\sqrt{4a-3(b+1)^2}}{2a},-b\frac{(b+1)+\sqrt{4a-3(b+1)^2}}{2a}\right).$$

We will now observe what happens for $\Delta_2=0$.
If $\Delta_2=0$, then equation (3.7) has one solution $x=\frac{2}{3}\frac{1}{b+1}$ and in a consequence (3.5) has one solution given by:

$$(x,y)=\left(\frac{2}{3}\frac{1}{b+1},-\frac{2}{3}\frac{b}{b+1}\right).$$

On the other hand, when $\Delta_2=-3(b+1)^2+4a=0$, then determinant in theorem 7 is $\Delta_1=(b+1)^2+4a=4(b+1)^2>0$. Hence we obtain two fixed points, which are equal to:

$$(x,y)=\left(\frac{2}{3}\frac{1}{b+1},-\frac{2}{3}\frac{b}{b+1}\right)$$

and

$$(x,y)=\left(\frac{-2}{(b+1)^2},\frac{2b}{(b+1)^2}\right).$$

In the result the solutions of (3.5), in case $\Delta_2=0$, are the fixed points of $H(x,y)$.

Now we will investigate what happens when $b=-1$. If $b=-1$, then (3.4) takes the form:

$$\begin{cases} x=1-a(1-ax^2+y)^2+x \\ y=1-ax^2+y, \end{cases} \tag{3.8}$$

If $a>0$ the solution of (3.8) are four points: $(x,y)=\left(\frac{1}{\sqrt{a}},\frac{1}{\sqrt{a}}\right)$, $(x,y)=\left(-\frac{1}{\sqrt{a}},\frac{1}{\sqrt{a}}\right)$, $(x,y)=\left(\frac{1}{\sqrt{a}},-\frac{1}{\sqrt{a}}\right)$ and $(x,y)=\left(-\frac{1}{\sqrt{a}},-\frac{1}{\sqrt{a}}\right)$. According to theorem 7 $(x,y)=\left(\frac{1}{\sqrt{a}},\frac{1}{\sqrt{a}}\right)$, $(x,y)=\left(-\frac{1}{\sqrt{a}},-\frac{1}{\sqrt{a}}\right)$ are the fixed points of $H(x,y)$. Hence $(x,y)=\left(\frac{1}{\sqrt{a}},-\frac{1}{\sqrt{a}}\right)$ and $(x,y)=\left(-\frac{1}{\sqrt{a}},-\frac{1}{\sqrt{a}}\right)$ is a period-two orbit of $H(x,y)$.
If $a<0$, then (3.8) has no solution.

□

Remark 6. *We may notice that the results of theorems 9 and 10 indeed corresponds with each other. Hence the relation* $a = \frac{3}{4}(1+b)^2$ *is also sufficient condition for period doubling.*

Theorem 11. *The eigenvalues of the Jacobian matrix of* $H^2(x,y)$ *fulfils the following relations:* $\lambda_1 + \lambda_2 = -2b + 4a^2x(1-ax^2+y)$ *and* $\lambda_1\lambda_2 = b^2$.

Proof. Let $(x,y) \in \mathbb{R}^2$.
Firstly let us observe that $H^2(x,y) = (1 - a(1-ax^2+y)^2 - bx, -b(1-ax^2+y))$.
In order to obtain the eigenvalues of $\mathbf{DH}^2(x,y)$ we are seeking for the roots of the function $\det(\mathbf{DH}^2(x,y) - \lambda\mathbb{I})$:

$$\det(\mathbf{DH}^2(x,y) - \lambda\mathbb{I}) = \det\begin{pmatrix} 4a^2x(1-ax^2+y) - b - \lambda & -2a(1-ax^2+y) \\ 2abx & -b-\lambda \end{pmatrix} =$$

$$= \left(4a^2x(1-ax^2+y) - b - \lambda\right)(-b-\lambda) + 4a^2bx(1-ax^2+y) =$$

$$= \lambda^2 + (2b - 4a^2x(1-ax^2+y))\lambda + b^2 = 0$$

Therefore using the Vieta's formulas we get that: $\lambda_1 + \lambda_2 = -2b + 4a^2x(1-ax^2+y)$ and $\lambda_1\lambda_2 = b^2$.

□

Theorem 12. *Let* $a \neq 0$.
If period doubling bifurcation connected with emerging of period 4 orbit occurs for $H(x,y)$*, then it takes place for* a, b *fulfilling the relation* $a = (b+1)^2 + \frac{1}{4}(b-1)^2$.

Proof. Let λ_1 and λ_2 be the eigenvalues of $\mathbf{DH}^2(x,y)$. Taking $\lambda_1 = -1$ and using the theorem 11 we obtain the following relation:

$$(b-1)^2 + 4a^2x(1-ax^2+y) = 0 \tag{3.9}$$

According to theorem 10 if (x,y) is a point belonging to period 2 orbit, then

$$(x,y) = \left(\frac{(b+1) + \sqrt{4a - 3(b+1)^2}}{2a}, -b\frac{(b+1) - \sqrt{4a-3(b+1)^2}}{2a}\right) \tag{3.10}$$

or

$$(x,y) = \left(\frac{(b+1) - \sqrt{4a - 3(b+1)^2}}{2a}, -b\frac{(b+1) + \sqrt{4a - 3(b+1)^2}}{2a} \right). \quad (3.11)$$

Now putting (3.10) into (3.9) we obtain the following relation of the parameters a and b:

$$a = (b+1)^2 + \frac{1}{4}(b-1)^2 \quad (3.12)$$

The same result ($a = (b+1)^2 + \frac{1}{4}(b-1)^2$) is obtained when we substitute (3.11) into (3.9).

□

Remark 7. *According to further numerical analyses we know that for $H(x,y)$ a period doubling connected with emerging of period* 4 *orbit occurs, hence the relation $a = (b+1)^2 + \frac{1}{4}(b-1)^2$ obtained in theorem 12 is also sufficient condition for period doubling.*

Further composing of the function $H(x,y)$ and finding its periodic points would be very problematic. That is why a software AUTO-07p was used to present relations between parameters a and b corresponding to further period doubling (figure 6 and figure 7). Let us notice that according to theorem 6 the interesting interval from the point of view of attracting sets for parameter b is $(-1,1)$. According to the numerical analysis for $b \in (-1,1)$ period-doubling is connected with successive emerging and fading of attracting periodic orbit.

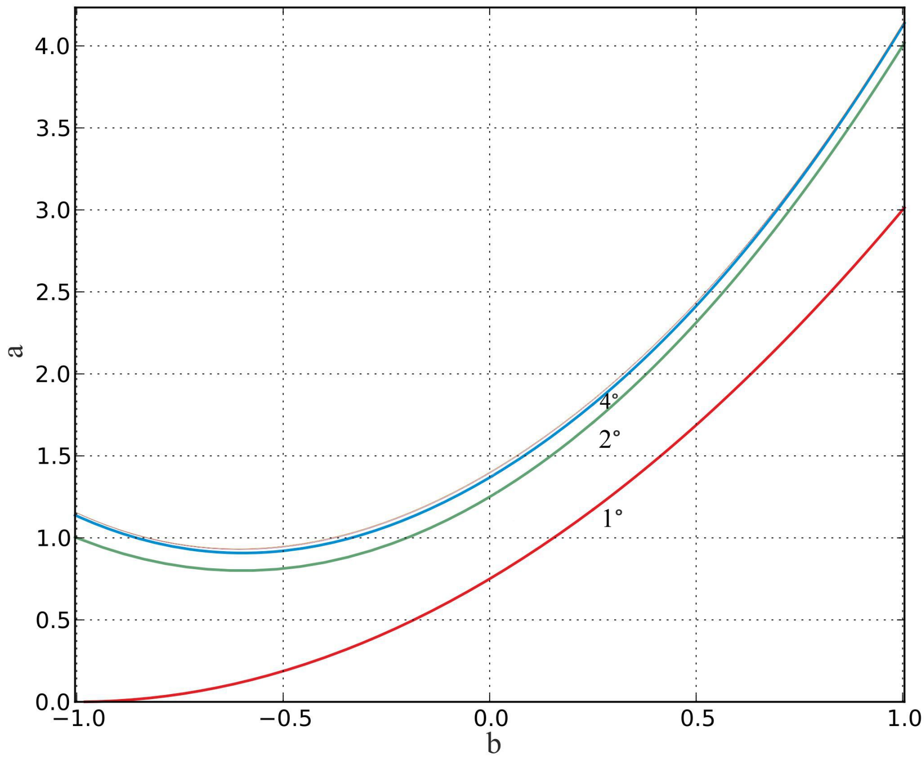

Figure 6. *State diagram of the Hénon map in (b,a) space.* 1^0, 2^0, 4^0 *indicate areas, where attracting fixed point and attracting orbits of period 2 and 4 exist.*

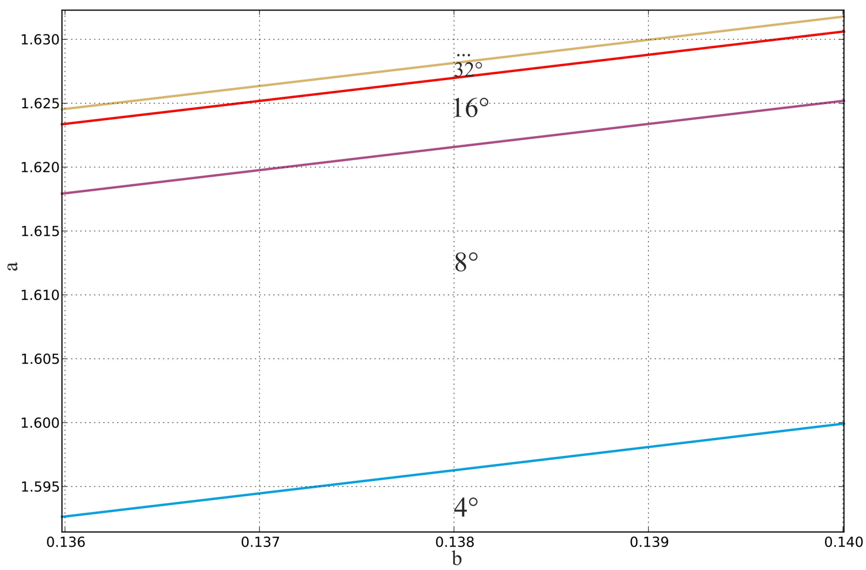

Figure 7. *Enlarged view for* $b \in [0.136, 1.4]$ *of the figure 6.* 4^0, 8^0, 16^0, 32^0 *indicate areas, where attracting orbits of period 4, 8, 16 and 32 exist.*

Let us choose $b \in (-1, 1)$. Increasing the parameter a we would find parameter a_1 such that period 2 orbit bifurcates from an attracting point. The value $a_1 = \frac{3}{4}(b+1)^2$ was analytically found in the theorem 9 and it is a first value of a, where period doubling occurs. Raising the parameter a we would find $a_2 > a_1$ such that period 2 orbit stops being attracting orbit, however attracting period 4 orbit emerge. According to the theorem 12 $a_2 = (b+1)^2 + \frac{1}{4}(b-1)^2$. The next value of parameter a would be $a_3 > a_2$, where period 4 orbit stops being attracting and attracting period 8 orbit appears. This way we would create an infinity sequence of $(a_n)_{n\in\mathbb{N}}$.

In 1978 mathematical physicist Mitchell Jay Feigenbaum discovered that the quotient

$$\frac{a_{n-1} - a_{n-2}}{a_n - a_{n-1}}$$

tends to 4.669201609... as n increases. The number 4.669201609... is known as Feigenbaum's constant. The most surprising fact about that number is its universality. The Feigenbaum's constant is the same for a wide range of one-parameter maps, where period doubling occurs (e.g. logistic map - example 2), and also for the Hénon map. [3]

The important consequence of existing of Feigenbaum's constant is the fact that the sequence $(a_n)_{n\in\mathbb{N}}$ has a limit a_∞. What is more, at a_∞ the chaotic behaviour of the map occurs.

Remark 8. *Before we will start to examine bifurcation diagrams for $H(x, y)$ with $b \neq 0$ it is important to notice (easily from the form of $H(x, y)$) that if we detect:*

- *a fixed point of the projection on x-axis of the orbit under $H(x, y)$, then the orbit considered in $\mathbb{R}^2$ is a fixed point;*
- *a period orbit of the projection on x-axis of the orbit under $H(x, y)$, then the orbit considered in $\mathbb{R}^2$ is periodic;*
- *a chaotic orbit of the projection on x-axis of the orbit under $H(x, y)$, then the orbit considered in $\mathbb{R}^2$ is chaotic.*

Example 3. *Obtaining an approximate value of Feigenbaum's constant for b=0.138.*

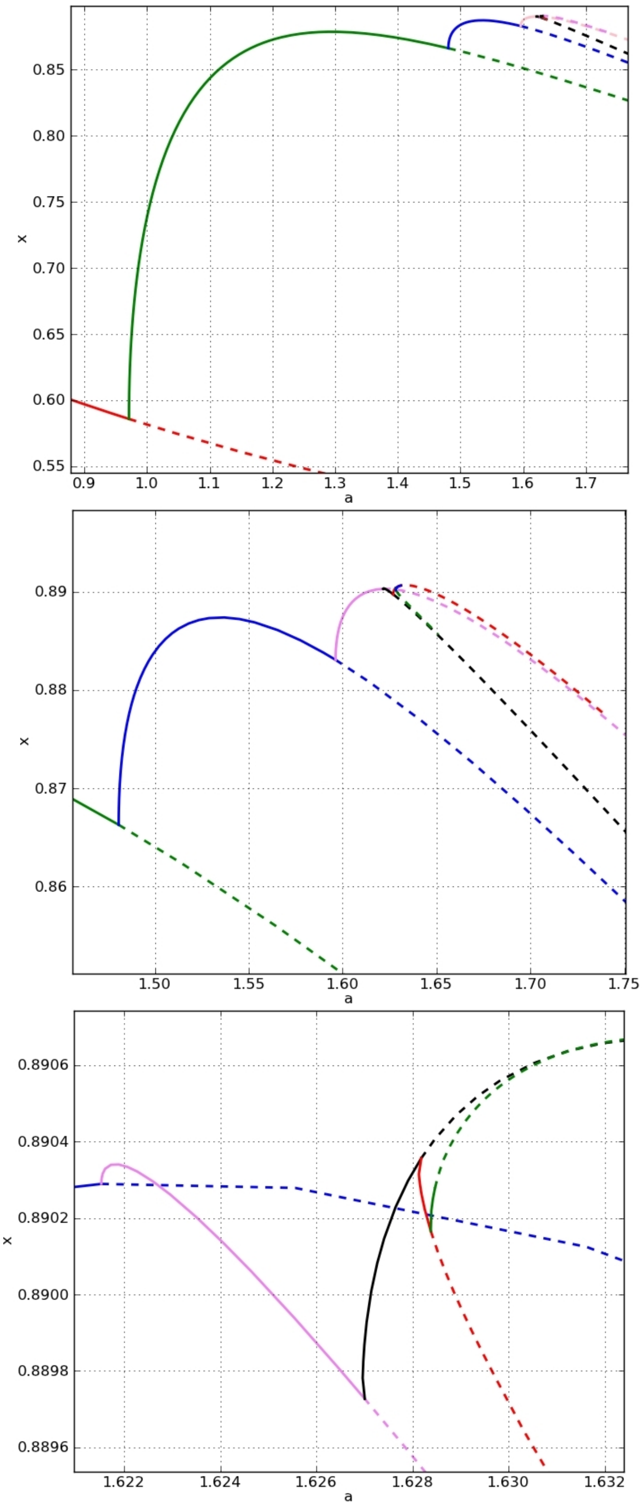

Figure 8. *One branch of bifurcation diagram for* $b = 0.138$. *The continuous line indicates stable (attracting) orbit and dotted line indicates unstable (non-attracting) orbit.*

According to theorem 9 the first value of a where period doubling occurs is $a_1 = \frac{3}{4}(1+b)^2 = \frac{3}{4}(1+0.138)^2 = 0.971283$. *Using theorem 12 we obtain that* $a_2 = (b+1)^2 + \frac{1}{4}(b-1)^2 = (0.138+1)^2 + \frac{1}{4}(0.138-1)^2 = 1.480805$. *We may observe that this result correspond with figure 8. Figure 8 was created with software AUTO-07p. Moreover with this program the further bifurcation values (from* a_3 *to* a_8*) were obtained. They are presented in the following table together with computed quotient* $\dfrac{a_{n-1}-a_{n-2}}{a_n-a_{n-1}}$.

n	a_n	$\dfrac{a_{n-1}-a_{n-2}}{a_n-a_{n-1}}$
3	*1.5962728169*	*4.41267544*
4	*1.6215738572*	*4.56375768*
5	*1.6269794670*	*4.68051547*
6	*1.6281462245*	*4.63301911*
7	*1.6283830630*	*4.92638443*
8	*1.6284686426*	*2.76746444*

Therefore obtained results are initially close to Feigenbaum's constant till the computing the quotient $\dfrac{a_5-a_4}{a_6-a_5}$. *For further calculation* $\dfrac{a_{n-1}-a_{n-2}}{a_n-a_{n-1}}$ *differ severely from* 4.669201609..., *because of the approximation of* a_6, a_7 *and* a_8.

Chapter 4

The coupled Hénon maps

In this chapter we will consider three bidirectionally coupled bistable Hénon maps.

4.1 Model

For the Hénon map there exist the area, where another period-doubling exists. That period doubling is connected with an attracting period 3 orbit, which bifurcates and looses its stability, but a new attracting period 6 orbit emerges and so on. Previously considered period doubling, connected with a fixed point, exists for every $b \in \mathbb{R}$. Period 3 orbit exists only for a certain b (surely for $b \in (0.134, 0.142)$ as it may be observed in Figure 9). Figure 9 shows that those periodic orbits coexist. This phenomenon of coexisting of two attractors is called bistability. Bistability is the special case of multistability, i.e., the coexistence of n attractors.

In order to choose three different bistable Hénon maps, which parameters differ slightly, state diagram created with AUTO-07p was used.

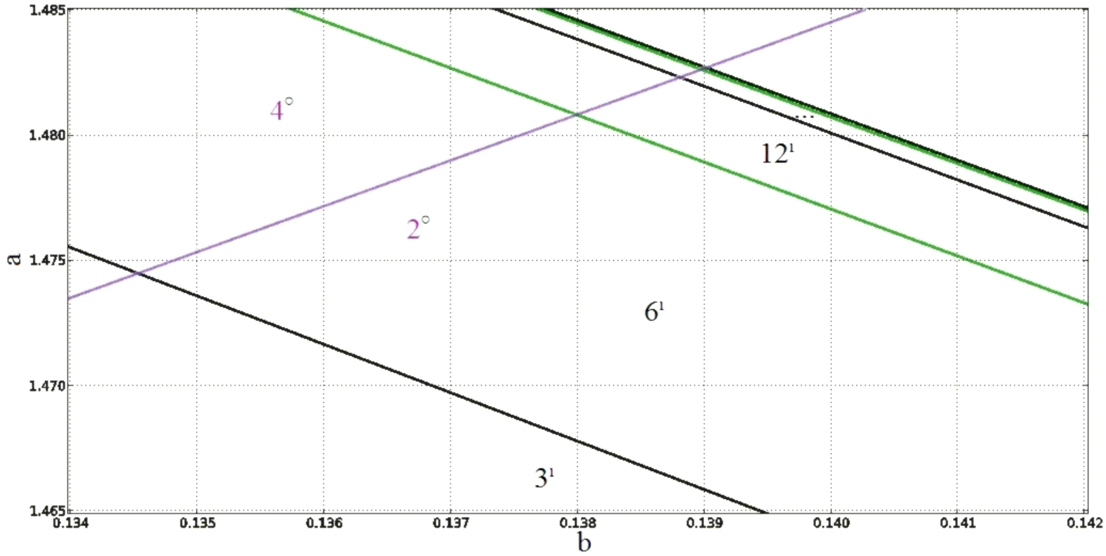

Figure 9. *State diagram of the Hénon map in (b,a) space.* 2^0, 4^0 *indicate attracting orbits of period 2 and 4.* $3^1, 6^1, 12^1$ *indicate attracting orbits of period 3, 6 and 12.*

The parameter $b = 0.138$ was chosen for all three maps. To choose three different values of parameter a in such a way to create three different bistable maps the following bifurcation diagrams of Figure 10 have been analysed.

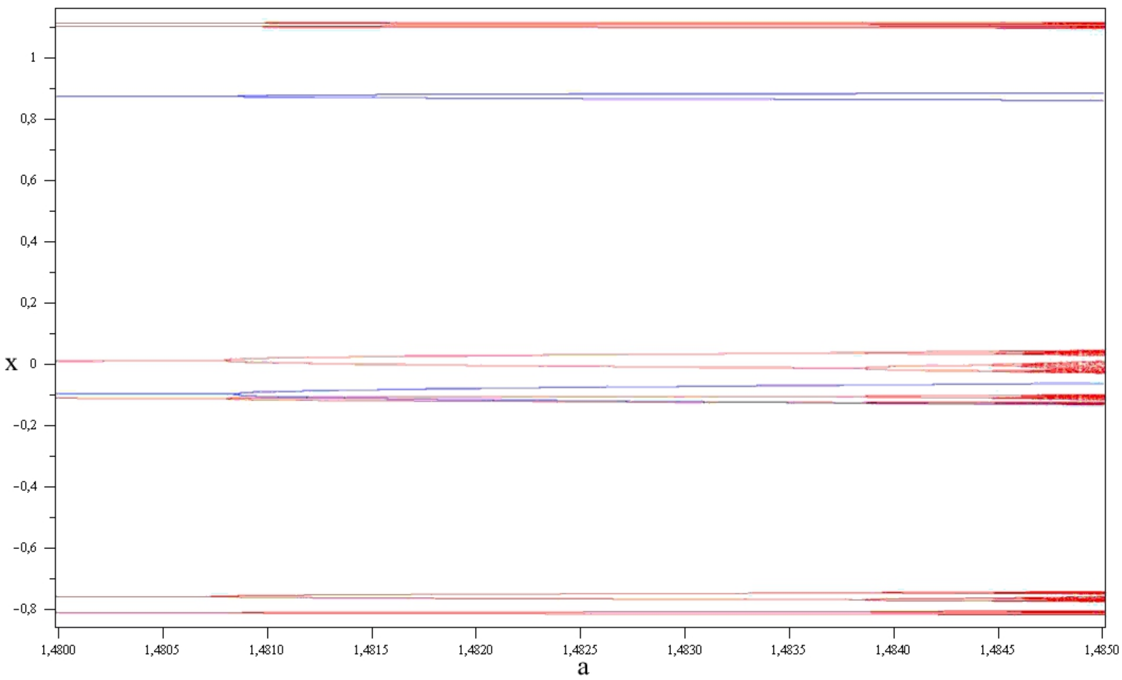

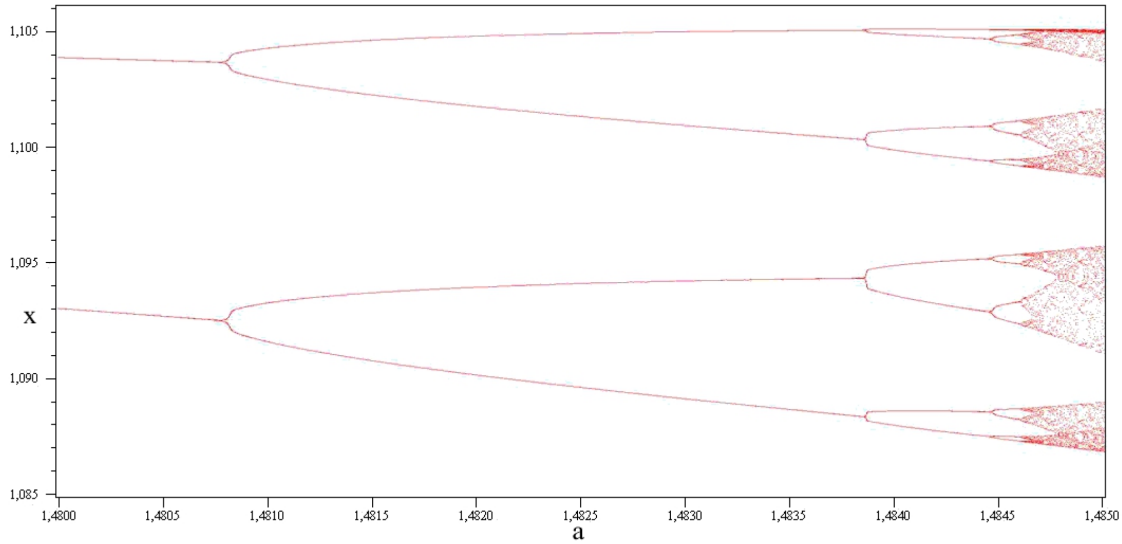
1,105
1,100
1,095
x
1,090
1,085
1,4800
1,4805
1,4810
1,4815
1,4820
1,4825
1,4830
1,4835
1,4840
1,4845
1,4850
a

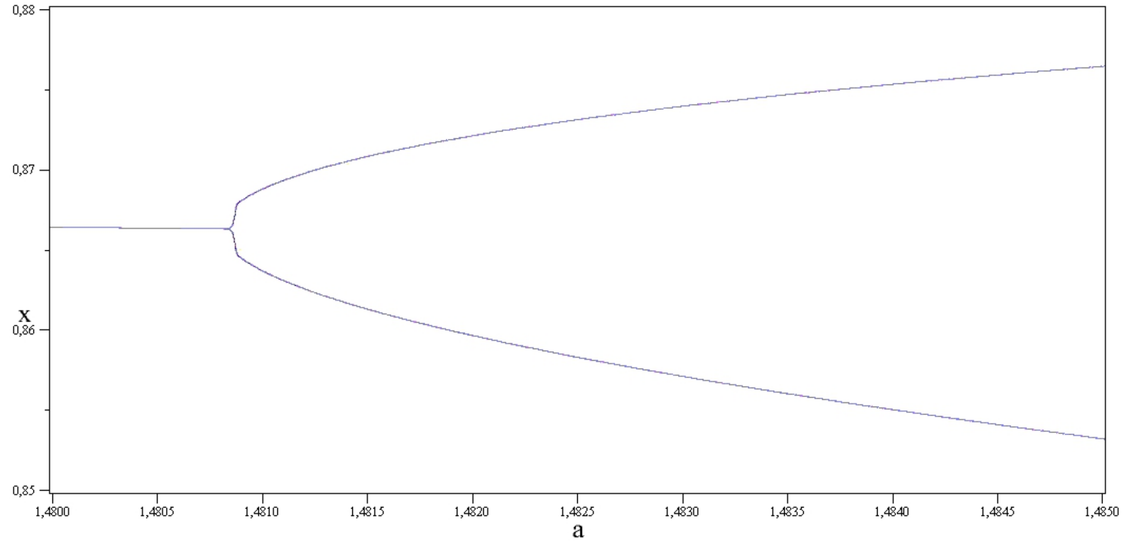
0,88
0,87
x
0,86
0,85
1,4800
1,4805
1,4810
1,4815
1,4820
1,4825
1,4830
1,4835
1,4840
1,4845
1,4850
a

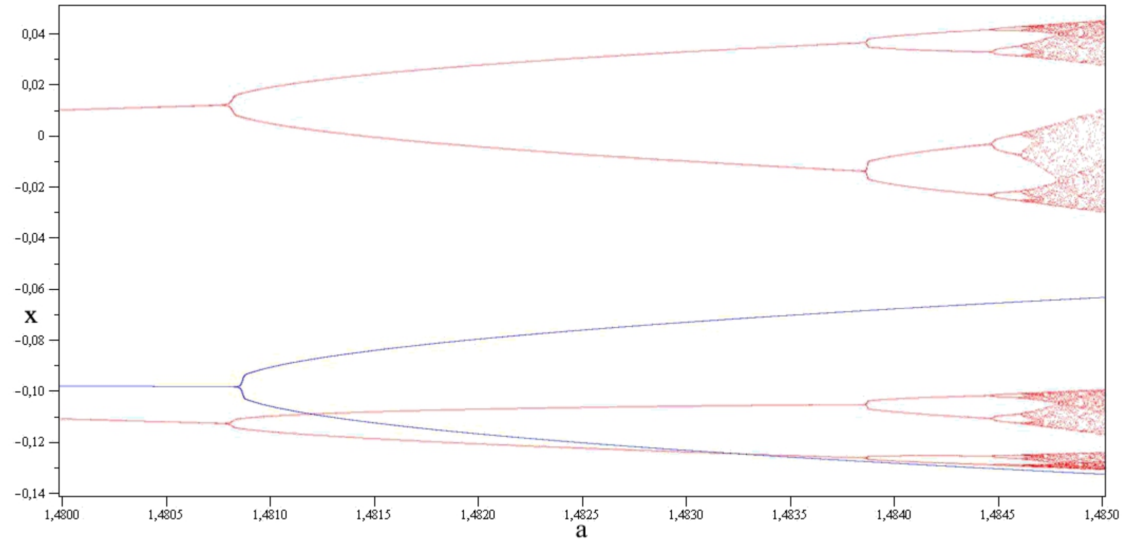
0,04
0,02
0
−0,02
−0,04
−0,06
x
−0,08
-0,10
−0,12
−0,14
1,4800
1,4805
1,4810
1,4815
1,4820
1,4825
1,4830
1,4835
1,4840
1,4845
1,4850
a

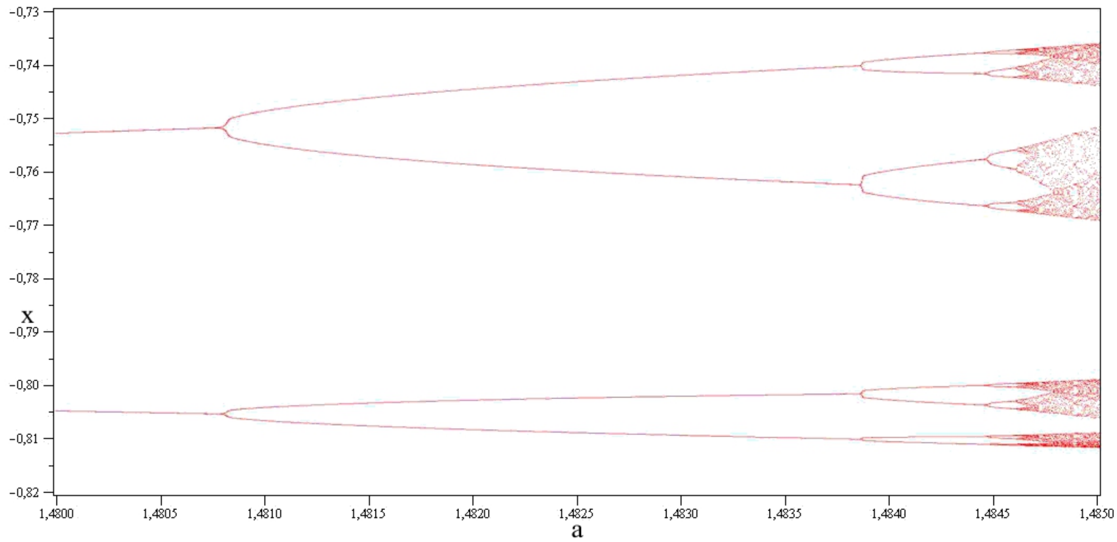

Figure 10. *Bifurcation diagrams and its enlargements for b=0.138 and a ∈ [1.48, 1.485]. Blue dots show bifurcation diagram with initial value in the basin of attraction of period 2 orbit and red dots represent bifurcation diagram with initial value in the basin of attraction of period 6 orbit.*

Notice that Figure 10 corresponds to Figure 9. According to this result the following bistable maps are considered in this chapter:

$$H_{2,6}(x, y) = (1 - 1.4807x^2 + y, -0.138x),$$

$$H_{4,12}(u, v) = (1 - 1.482u^2 + v, -0.138u),$$

$$H_{4,C}(w, z) = (1 - 1.4847w^2 + z, -0.138w).$$

Figure 11-13 show the basins of attraction for the maps $H_{2,6}(x, y)$, $H_{4,12}(u, v)$ and $H_{4,C}(w, z)$. These plots have been created using the software DYNAMICS FOR WINDOWS 2.

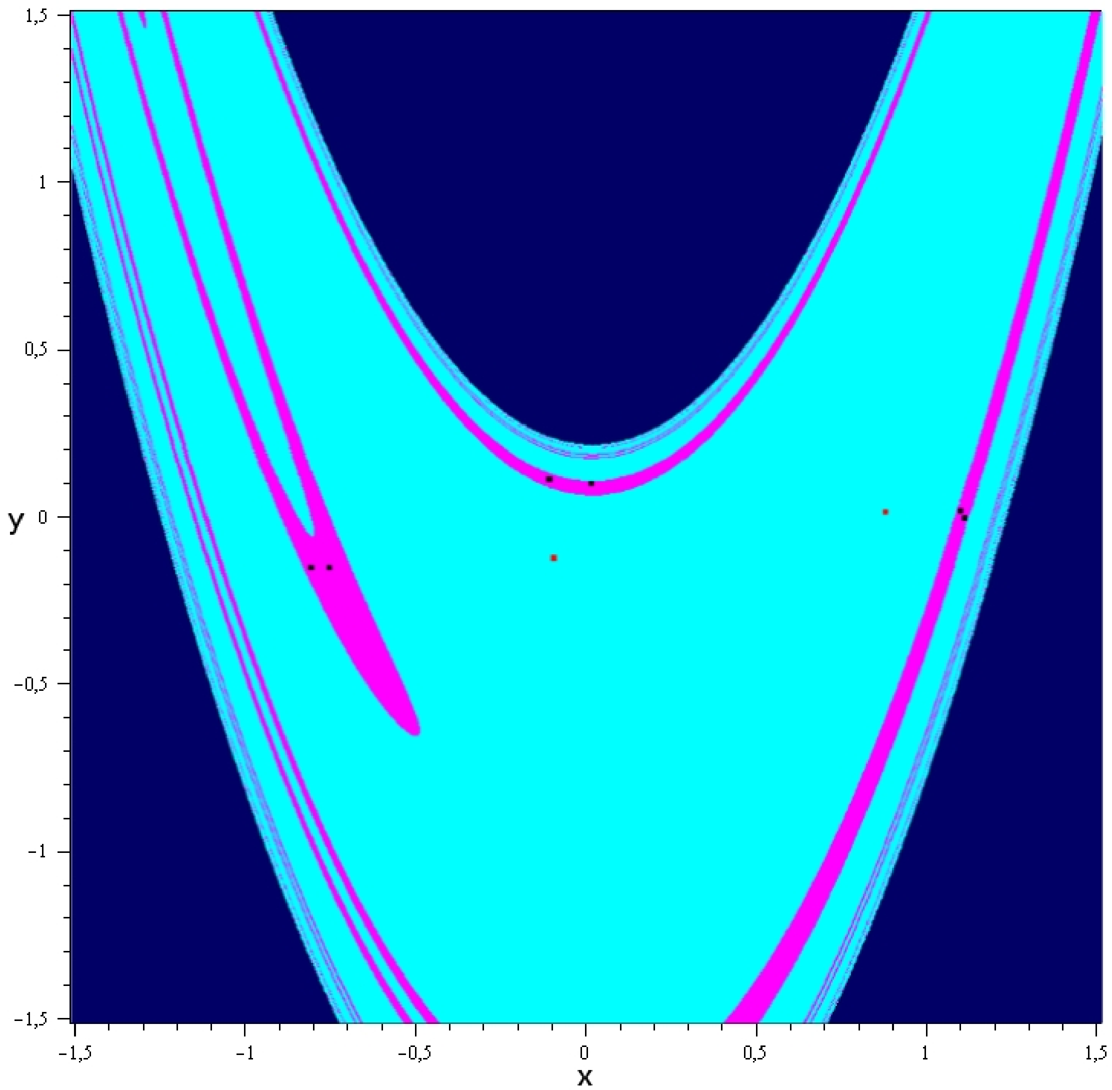

Figure 11. *Basins of attraction for the map* $H_{2,6}(x, y)$.

The cyan area is a basin of attraction of period 2 orbit (red dots), the pink area is a basin of attraction of period 6 orbit (black dots) and the navy blue area includes points, which diverge from the area of the picture (escape to infinity).

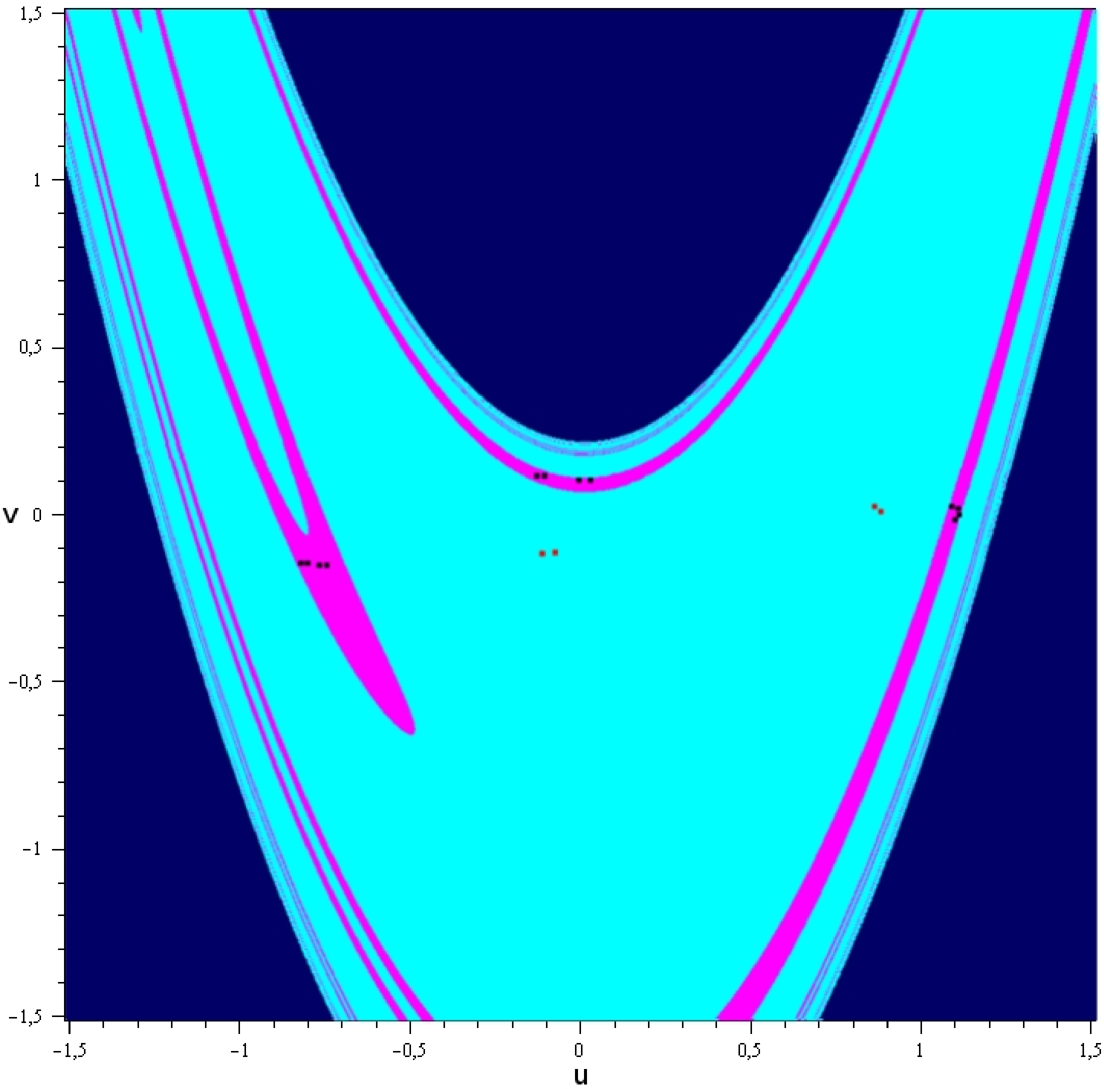

Figure 12. *Basins of attraction for the map* $H_{4,12}(u, v)$.

The cyan area is a basin of attraction of period 4 orbit (red dots), the pink area is a basin of attraction of period 12 orbit (black dots) and the navy blue area includes points, which diverge from the area of the picture (escape to infinity).

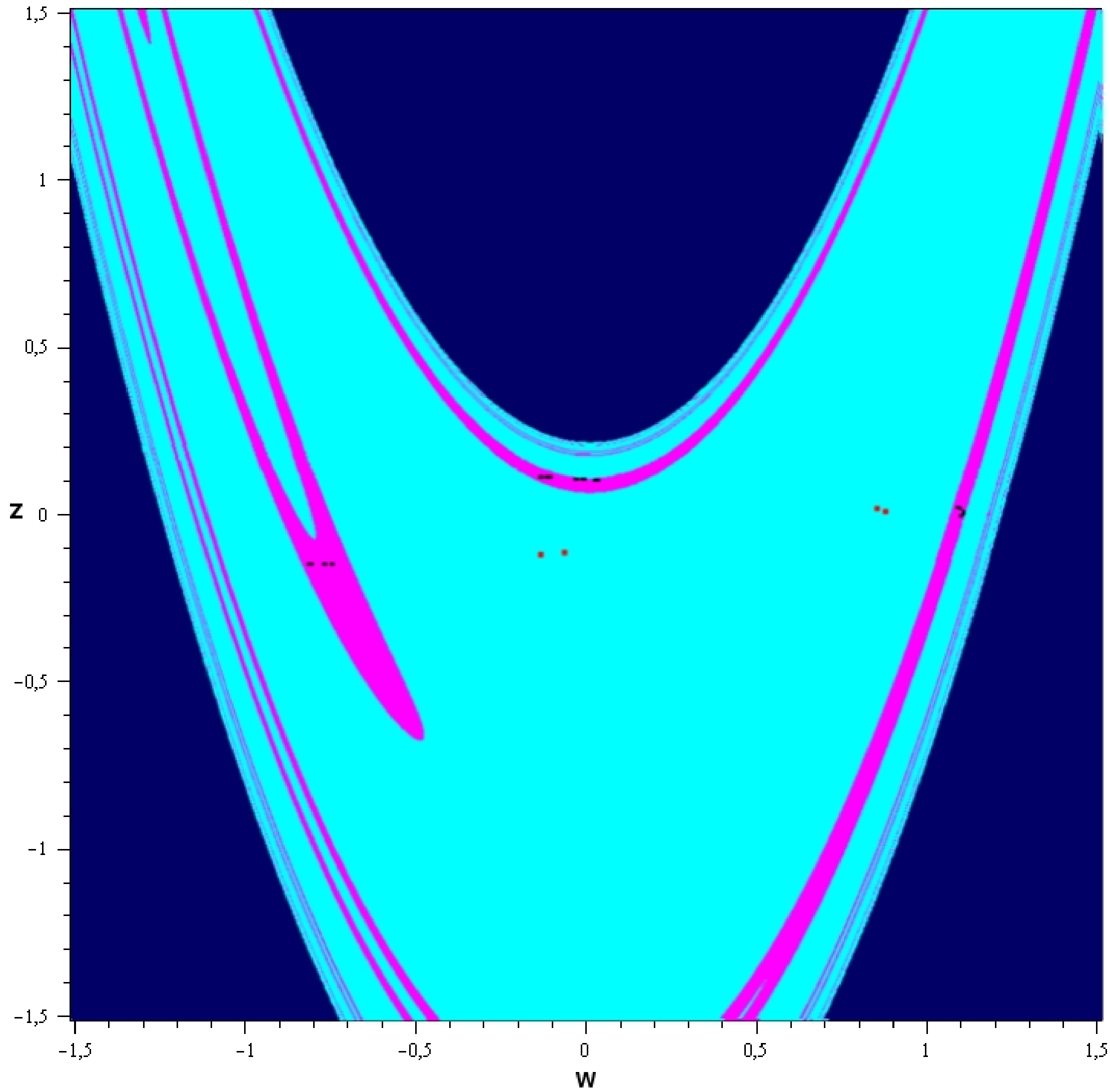

Figure 13. *Basins of attraction for the map* $H_{4,C}(w,z)$.
The cyan area is a basin of attraction of period 4 orbit (red dots), the pink area is a basin of attraction of chaotic attractor (black dots) and the navy blue area includes points, which diverge from the area of the picture (escape to infinity).

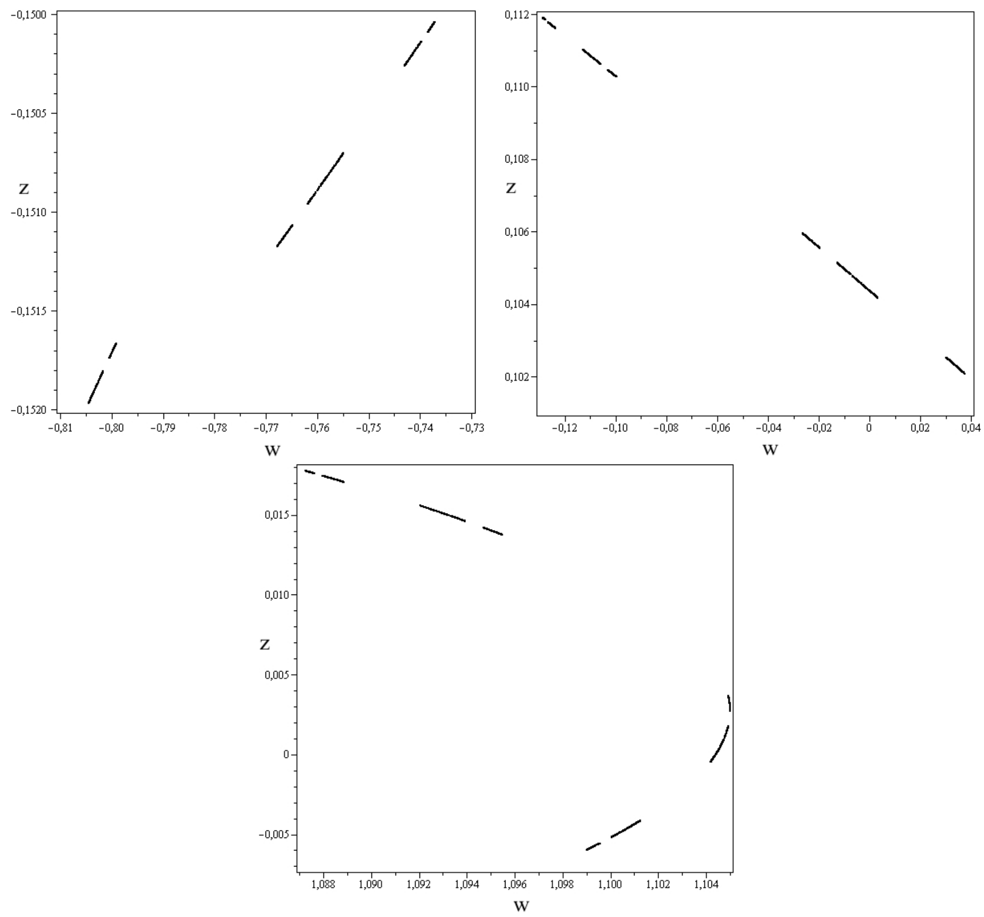

Figure 14. *Chaotic attractor occurring in $H_{4,C}(w,z)$.*

Now we will consider the bidirectional coupling of the chosen maps $H_{2,6}(x,y)$, $H_{4,12}(u,v)$ and $H_{4,C}(w,z)$ by introducing the coupling signals $\varepsilon(z-y)$, $\varepsilon(y-v)$ and $\varepsilon(v-z)$. Hence, we will obtain the following system:

$$\begin{cases} x_{n+1} = 1 - 1.4807x_n^2 + y_n + \varepsilon(z_n - y_n), \\ y_{n+1} = -0.138x_n, \\ u_{n+1} = 1 - 1.482u_n^2 + v_n + \varepsilon(y_n - v_n), \\ v_{n+1} = -0.138u_n, \\ w_{n+1} = 1 - 1.4847w_n^2 + z_n + \varepsilon(v_n - z_n), \\ z_{n+1} = -0.138w_n, \end{cases} \tag{4.1}$$

where ε ($\varepsilon \in [0,1]$) is the strength of coupling.

Remark 9. *If $\varepsilon = 0$, then $H_{2,6}(x,y)$, $H_{4,12}(u,v)$ and $H_{4,C}(w,z)$ are not coupled.*

4.2 Analyses of the coupling

Definition 23. *Synchronization is a process where two or more systems, which are either identical or non-identical, adjust a given property of their dynamics to a common behaviour due to coupling. [1]*

Throughout years of studying many different synchronization states were distinguished ([1], [10]), but we will focus on ideal synchronization and practical synchronization.

Definition 24. *Assuming that two systems are represented by two arbitrarily chosen orbits $\{x_n\}_{n\in\mathbb{N}}$, $\{y_n\}_{n\in\mathbb{N}}$, the* ***ideal synchronization*** *takes place when $\{x_n\}_{n\in\mathbb{N}}$, $\{y_n\}_{n\in\mathbb{N}}$ converge to the same value and remain in step with each other during further evolution (i.e., $\lim_{n\to\infty} x_n - y_n = 0$). [9]*

Definition 25. *Assuming that two systems are represented by two arbitrarily chosen orbits $\{x_n\}_{n\in\mathbb{N}}$, $\{y_n\}_{n\in\mathbb{N}}$, the* ***practical synchronization*** *means that for $\{x_n\}_{n\in\mathbb{N}}$, $\{y_n\}_{n\in\mathbb{N}}$ occurs $\lim_{n\to\infty} |x_n - y_n| \leq \delta$, where δ is small parameter. [9]*

Remark 10. *It is important to note that bifurcation diagrams presented in this section aren't reinitialized for each ε. It means that if for a certain parameter ε_1 the last iteration of x is equal to x_0, then for ε_2 calculated in the next step of procedure the initial value for x is equal to x_0. This way we may investigate the evolution of obtained attractor for increasing ε.*

Remark 11. *We say that more than two systems are synchronized if all systems are synchronized with each other.*

In this section we will analyse the behaviour of the system (4.1) with different initial values for $\varepsilon = 0$. Firstly we will consider the case, where $H_{2,6}(x, y)$ has its initial value on period 2 orbit, $H_{4,12}(u, v)$ has its initial value on period 4 orbit and $H_{4,C}(w, z)$ has its initial value on period 4 orbit. We will notice that the results varies depending on the initial position on attractor. The second considered case will be $H_{2,6}(x, y)$ with initial value on period 6 orbit, $H_{4,12}(u, v)$ with initial value on period 12 orbit and $H_{4,C}(w, z)$ with initial value on chaotic attractor.

Example 4. *$H_{2,6}$ in period 2, $H_{4,12}$ in period 4, $H_{4,C}$ in period 4*

We will analyse the bifurcation diagrams for the map (4.1) shown in Figure 15-17, where the coupling strength ε is the bifurcational parameter. For $\varepsilon = 0$ we start from the following initial conditions: $x_0 = 0.8665180648$, $y_0 = 0.01340043371$, $u_0 = 0.8720318149$, $v_0 = 0.01094848768$, $w_0 = 0.8760190573$ and $z_0 = 0.008883582048$.

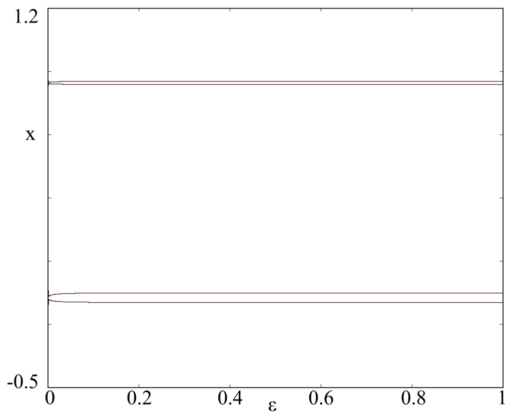

Figure 15. *The bifurcation diagram of variable x versus the coupling strength ε.*

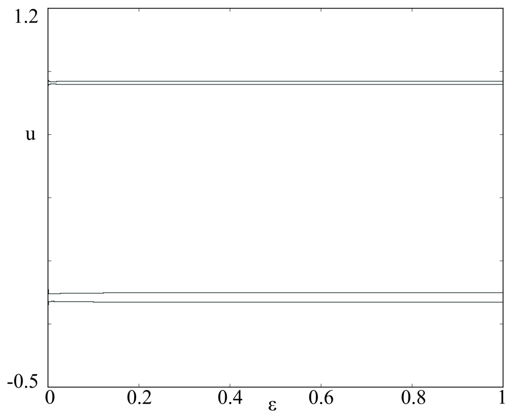

Figure 16. *The bifurcation diagram of variable u versus the coupling strength ε.*

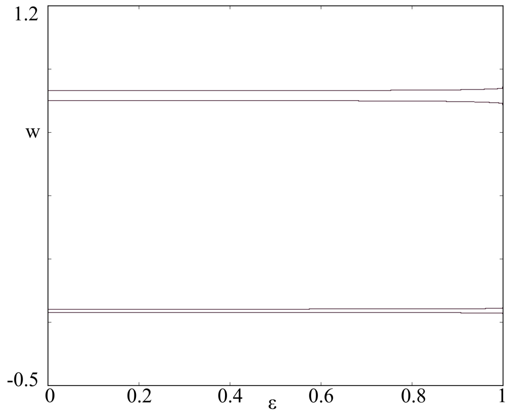

Figure 17. *The bifurcation diagram of variable w versus the coupling strength ε.*

In Figure 15 one can see that the period 2 orbit bifurcates to period 4 orbit for $\varepsilon > 0$.

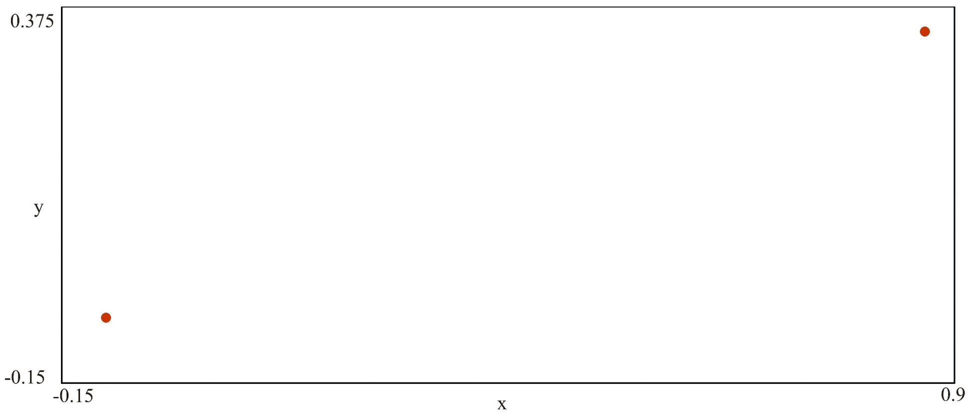

(a)

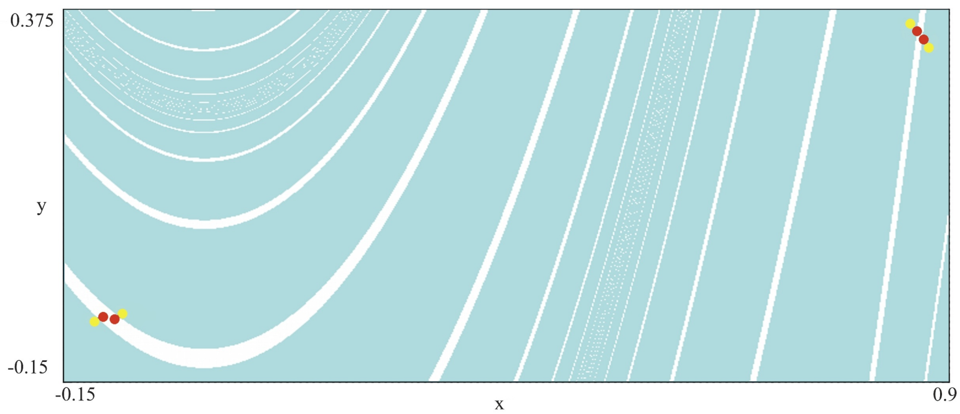

(b)

Figure 18. *The basins of attraction for $H_{2,6}(x, y)$ with (a) $\varepsilon = 0$ and (b) $\varepsilon = 0.001$.*

Figure 18(a) shows the basin of attraction (white area) of period 2 orbit (red dots) for $H_{2,6}(x, y)$ with $\varepsilon = 0$. Figure 18(b) presents the basin of attraction (white area) of the previous period 2 orbit, which have already bifurcated to period 4 orbit (red dots), for $H_{2,6}(x, y)$ with $\varepsilon = 0.001$. It is worth noting that in Figure 18(b) also another period 4 orbit emerges (yellow dots), which basin is shown as the turquoise area. As might be seen in Figure 16 and 17 period 4 orbits remain period 4 orbits, while ε is increased.

Now, we will consider the diagrams of the differences $x - u$, $u - w$ and $w - x$ versus the coupling strength ε in order to find synchronization.

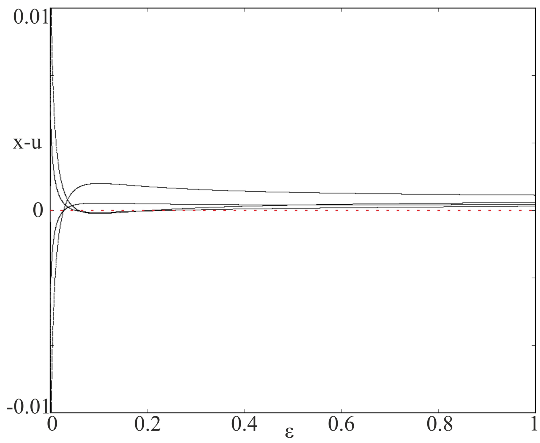

Figure 19. *The diagram of the difference $x - u$ versus the coupling strength ε.*

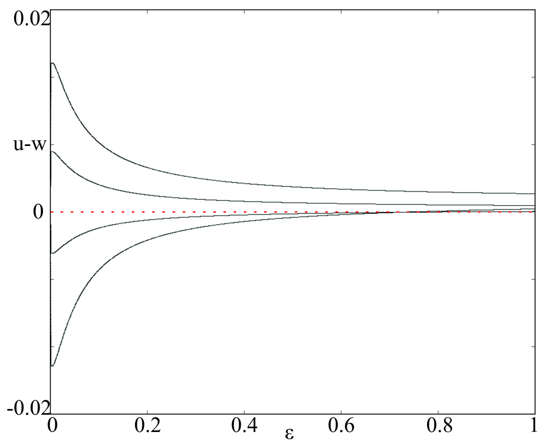

Figure 20. *The diagram of the difference $u - w$ versus the coupling strength ε.*

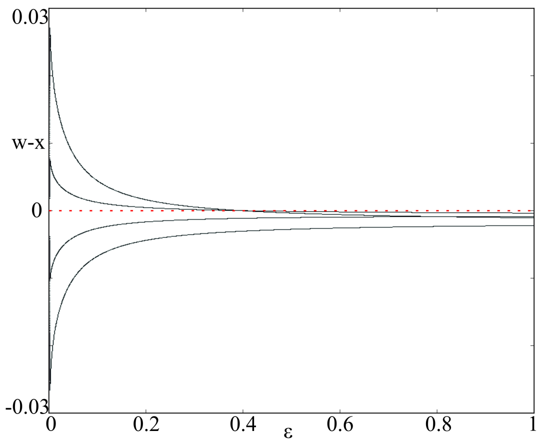

Figure 21. *The diagram of the difference $w - x$ versus the coupling strength ε.*

Analysing the above figures we may conclude that the considered maps are practically synchronized for $\varepsilon \in (0, 1]$, because for every $\varepsilon \in (0, 1]$ there exist $\delta \leq 0.028$ such that $\lim_{n\to\infty} |x_n - u_n| \leq \delta$, $\lim_{n\to\infty} |u_n - w_n| \leq \delta$ and $\lim_{n\to\infty} |w_n - x_n| \leq \delta$. What is more, it should be observed that $\delta = 0.028$ may be considered as small, because it is only approximately 3 percent of the range of x, u, w in Figure 15, 16 and 17.

In the further analysis we will considered the so-called Lyapunov exponents.

Definition 26. ***Lyapunov exponents*** *of the map* $f : \mathbb{R}^k \to \mathbb{R}^k$ *are numbers defined as:*

$$\lambda_i = \lim_{n\to\infty} \frac{1}{n} \ln|\sigma_i(n)|,$$

where $\sigma_i(n)$ *are eigenvalues of the matrix* $\boldsymbol{Df}^n(x_0)$.

There exists a set of k *Lyapunov exponents. Ordering the set* $\{\lambda_i\}$ $(i = 1, .., k)$ *according to less-equal relation we obtain so-called* ***spectrum of the Lyapunov exponents****. A simplified form of the set* $\{\lambda_i\}$ *is the* ***spectrum of the signs of Lyapunov exponents****, defined as a set of +, 0, -, which means positive, zero and negative values of the exponents* λ_i. *[10]*

According to [10] the following relation between spectrum of the signs of Lyapunov exponents and attractor type occurs:

Spectrum of the signs of Lyapunov exponents	Type of attracting set
(-, -, ..., -)	fixed point
(-, -, ..., -)	periodic orbit
(+, ..., +, -, ..., -)	chaotic attractor

Example 5. *$H_{2,6}$ in period 2, $H_{4,12}$ in period 4, $H_{4,C}$ in period 4*

Calculating the bifurcation diagrams of Figure 22-24 we start with the following initial conditions for $\varepsilon = 0$: $x_0 = 0.8665180648$, $y_0 = 0.01340043371$, $u_0 = -0.07933686728$, $v_0 = -0.1186399754$, $w_0 = -0.1304891380$ and $z_0 = -0.1208906299$.

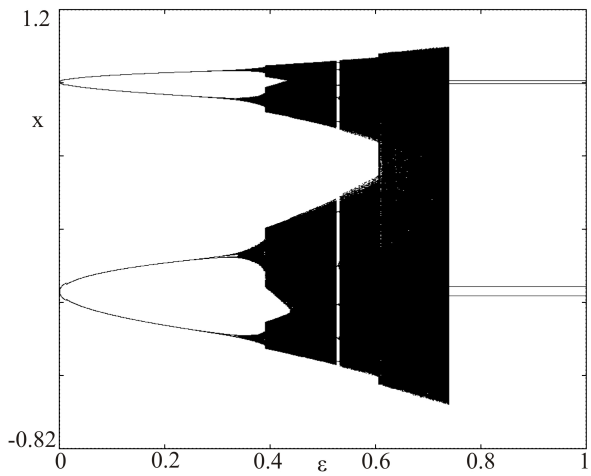

Figure 22. *The bifurcation diagram of variable x versus the coupling strength ε.*

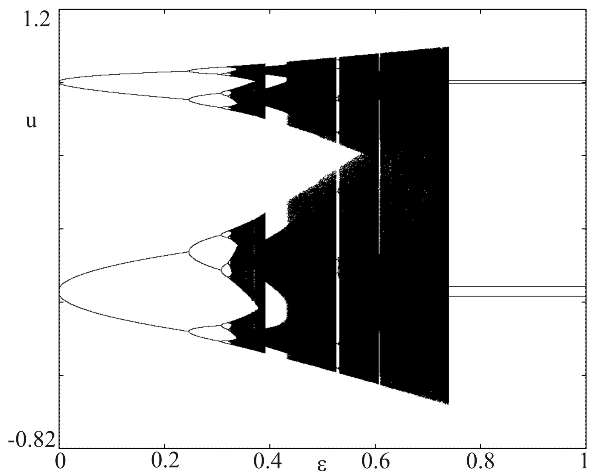

Figure 23. *The bifurcation diagram of variable u versus the coupling strength ε.*

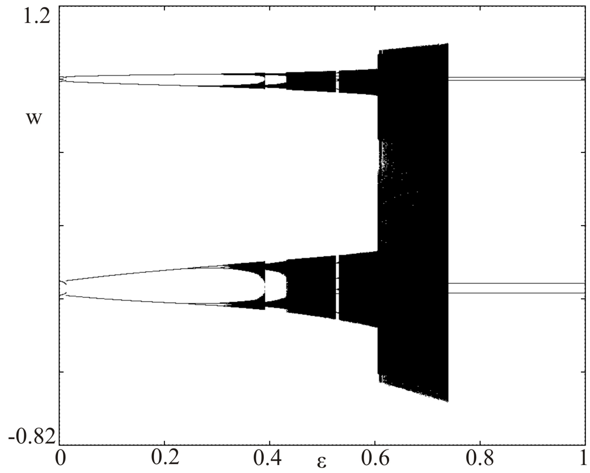

Figure 24. *The bifurcation diagram of variable w versus the coupling strength ε.*

Now, let us notice that Lyapunov exponents correspond system behaviour shown in Figure: 22, 23 and 24.

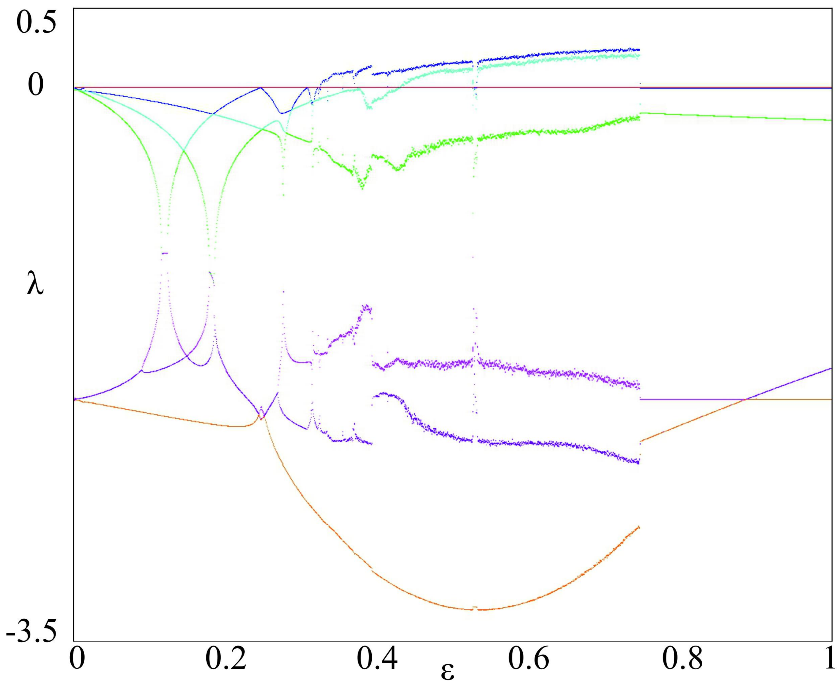

Figure 25. *The Lyapunov exponents versus the coupling strength ε. The red line indicate $\lambda = 0$.*

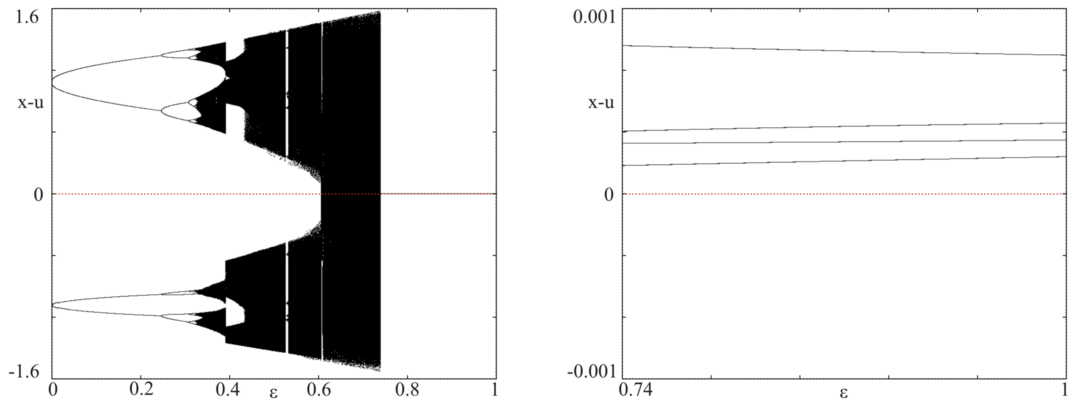

Figure 26. *The diagram of the difference $x - u$ versus the coupling strength ε.*

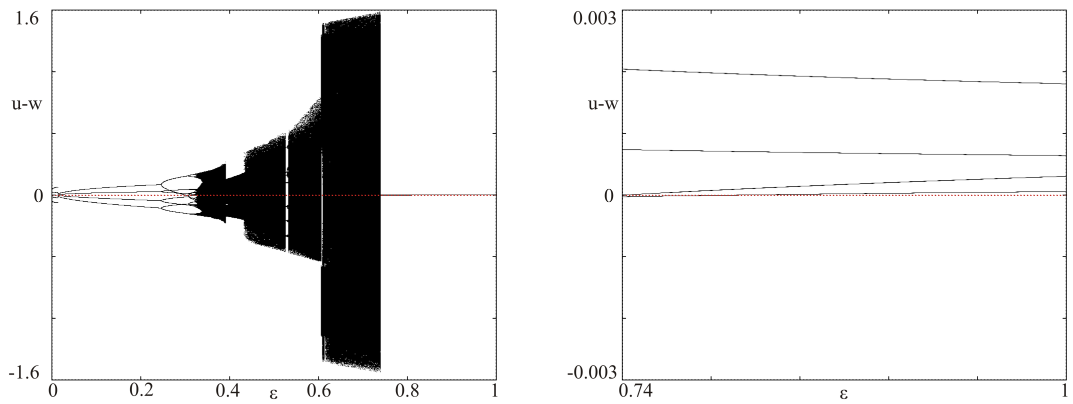

Figure 27. *The diagram of the difference $u - w$ versus the coupling strength ε.*

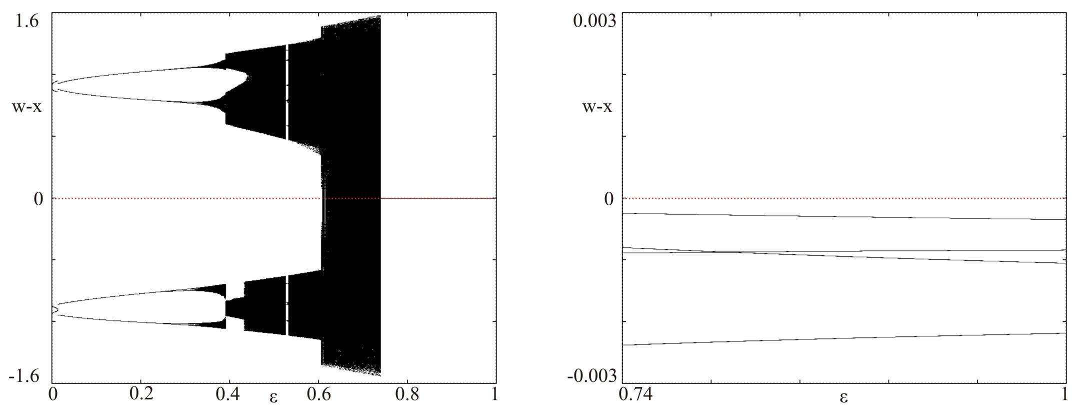

Figure 28. *The diagram of the difference $w - x$ versus the coupling strength ε.*

According to Figure 26, 27 and 28 we find $\varepsilon^* \approx 0.74$ *such that for every* $\varepsilon \in [\varepsilon^*, 1]$ *we obtain very effective practical synchronization with* $\delta \lesssim 0.0024$*. It is also worth noting that for* $\varepsilon \in (0, \varepsilon^*)$ *maps are not synchronized.*

Example 6. $H_{2,6}$ *in period 6,* $H_{4,12}$ *in period 12,* $H_{4,C}$ *in chaotic attractor*

Calculating the bifurcation diagrams of Figure 29-32 we start with the following initial conditions for $\varepsilon = 0$*:* $x_0 = 1.092584689$*,* $y_0 = 0.01542643645$*,* $u_0 = 1.090201829$*,* $v_0 = 0.01654230768$*,* $w_0 = 1.088825968$ *and* $z_0 = 0.01710160090$*.*

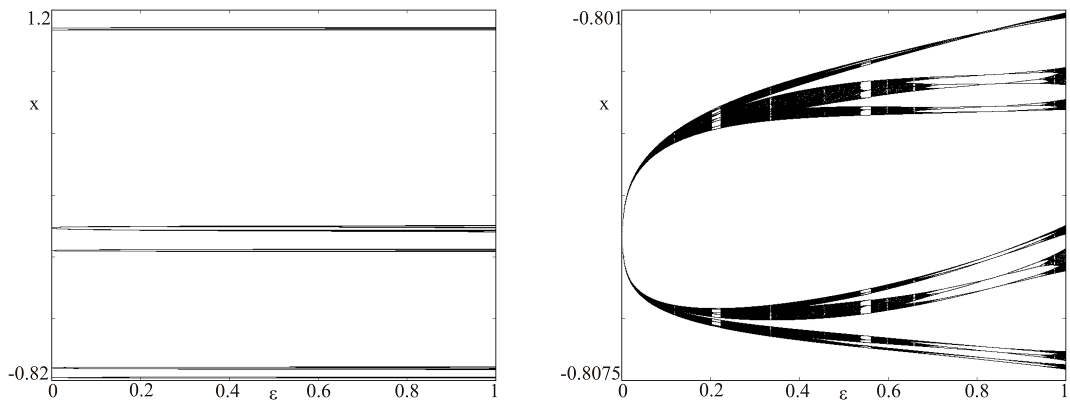

Figure 29. *The bifurcation diagram of variable* x *versus the coupling strength* ε*.*

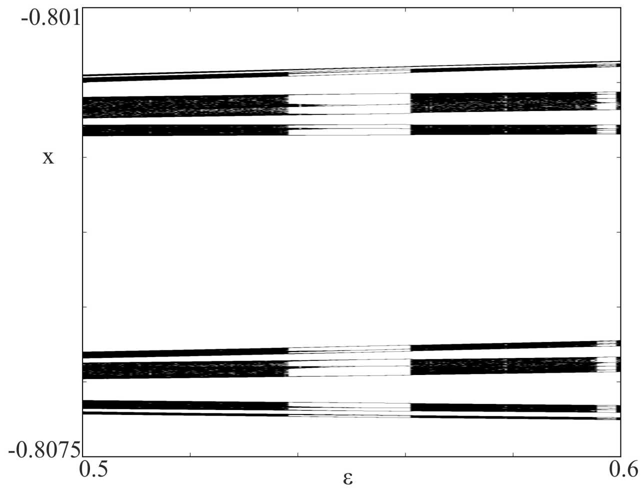

Figure 30. *Enlargement of Figure 29.*

In Figure 30 a set of parameter values, where periodic orbit occurs, might be observed. According to [3] it is so-called 'periodic window'.

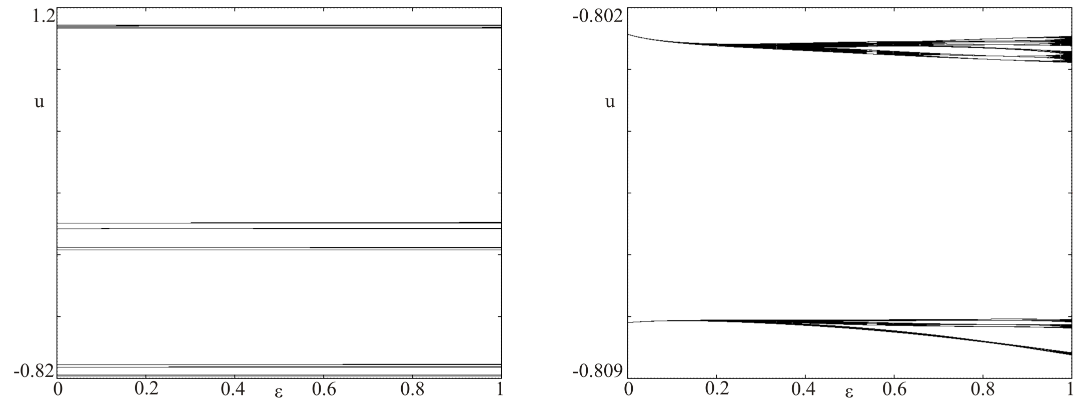

Figure 31. *The bifurcation diagram of variable u versus the coupling strength ε.*

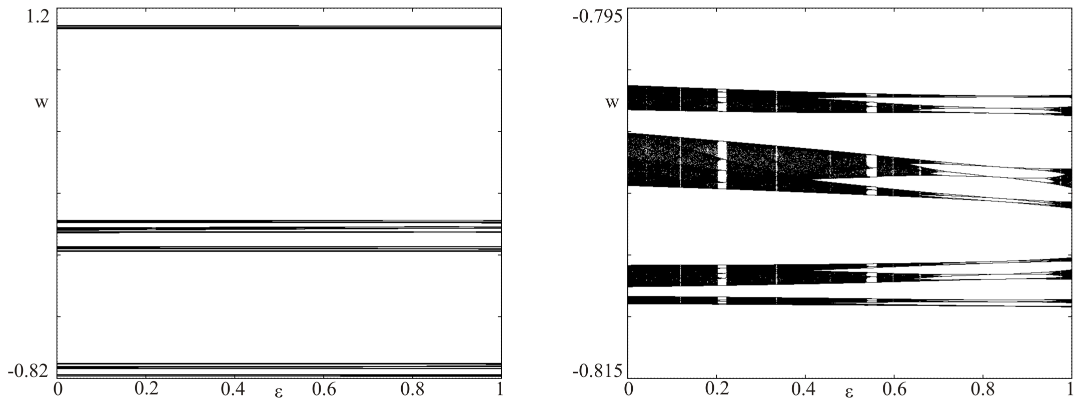

Figure 32. *The bifurcation diagram of variable w versus the coupling strength ε.*

We may observe that Figure 29, 31 and 32 present evolution of chaotic attractors with emerging 'periodic windows'.

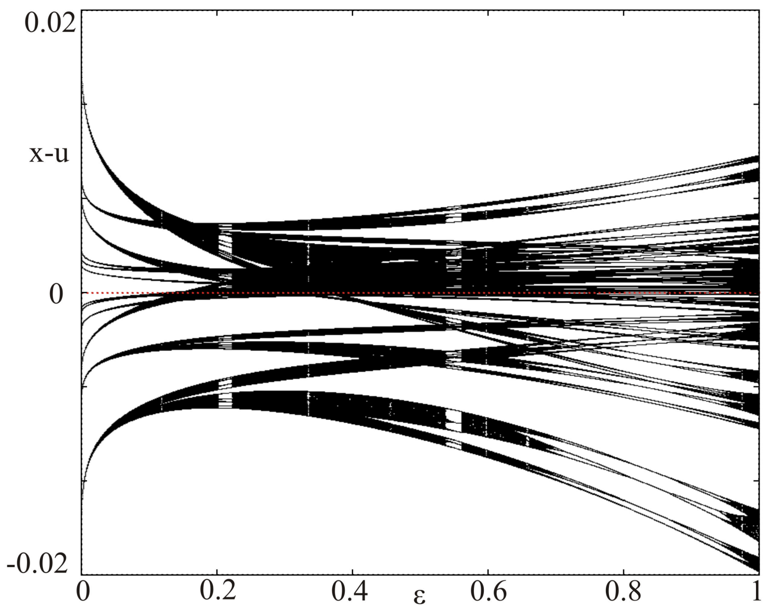

Figure 33. *The diagram of the difference $x - u$ versus the coupling strength ε.*

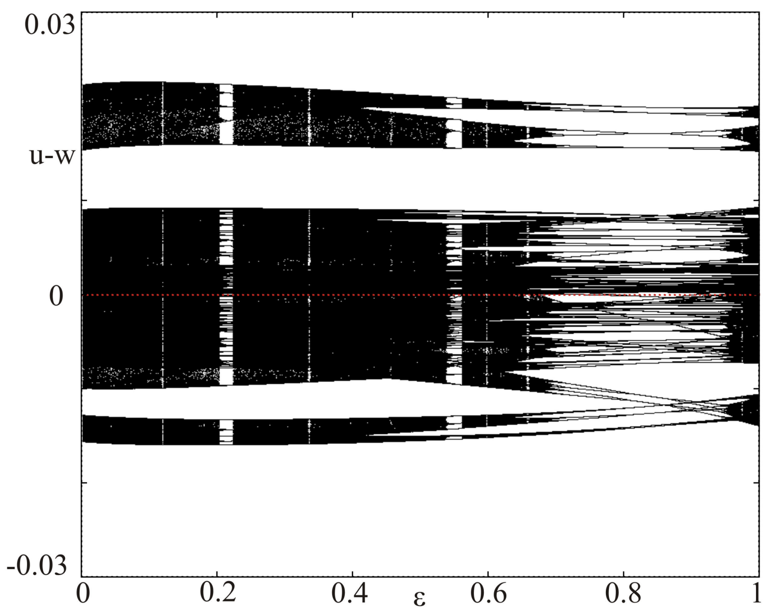

Figure 34. *The diagram of the difference $u - w$ versus the coupling strength ε.*

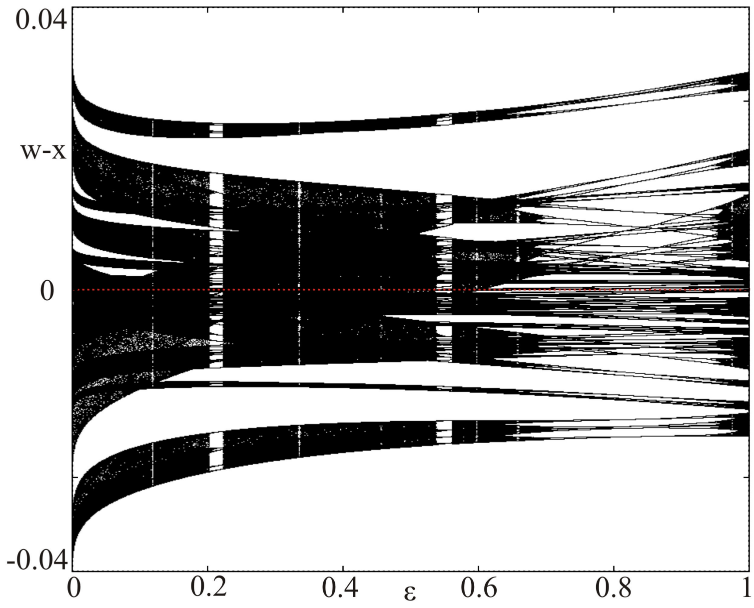

Figure 35. *The diagram of the difference $w - x$ versus the coupling strength ε.*

It may be observed that there occurs practical synchronization with $\delta \leq 0.04$, *which may be called small, because* $\delta = 0.04$ *is approximately 2 percent of the range of* x, u, w *in Figure 29, 31 and 32.*

Example 7. *$H_{2,6}$ in period 6, $H_{4,12}$ in period 12, $H_{4,C}$ in chaotic attractor*

Calculating the bifurcation diagrams of Figure 36-38 we start with the following initial conditions for $\varepsilon = 0$: $x_0 = -0.1117857714$, $y_0 = 0.1110876031$, $u_0 = -0.1064446881$, $v_0 = 0.1107446682$, $w_0 = 0.0305064123$ and $z_0 = 0.1025100836$.

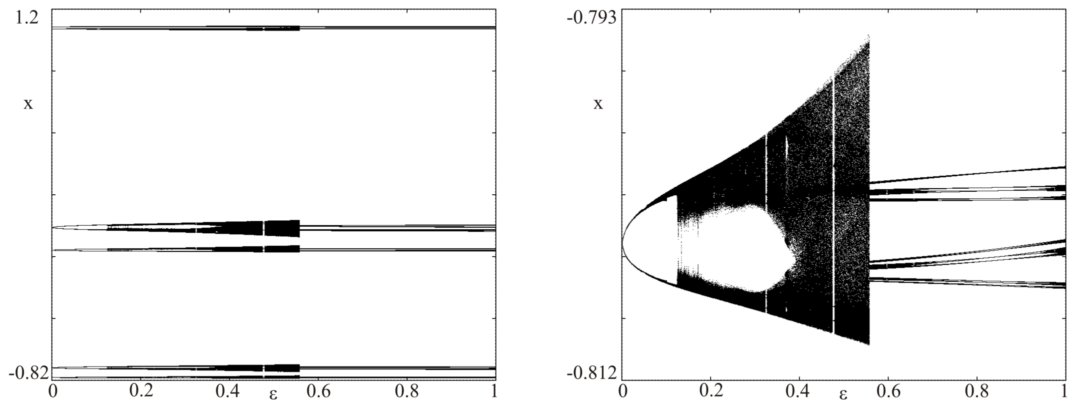

Figure 36. *The bifurcation diagram of variable x versus the coupling strength ε.*

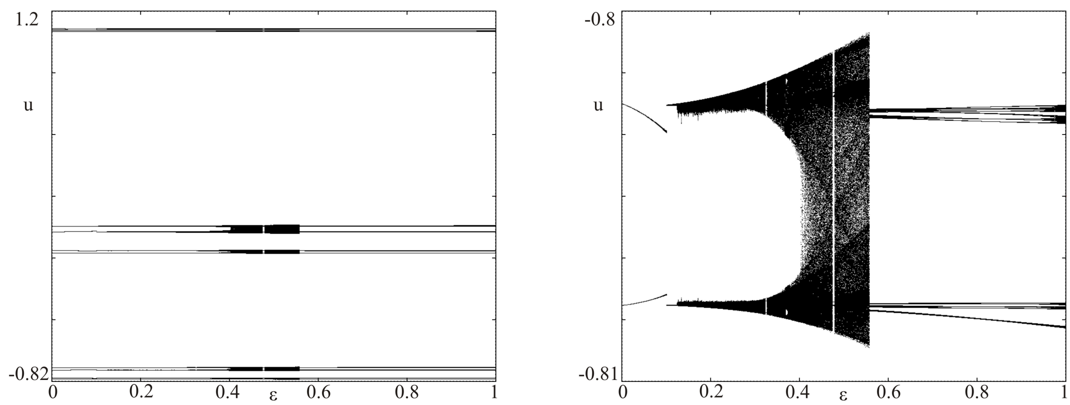

Figure 37. *The bifurcation diagram of variable u versus the coupling strength ε.*

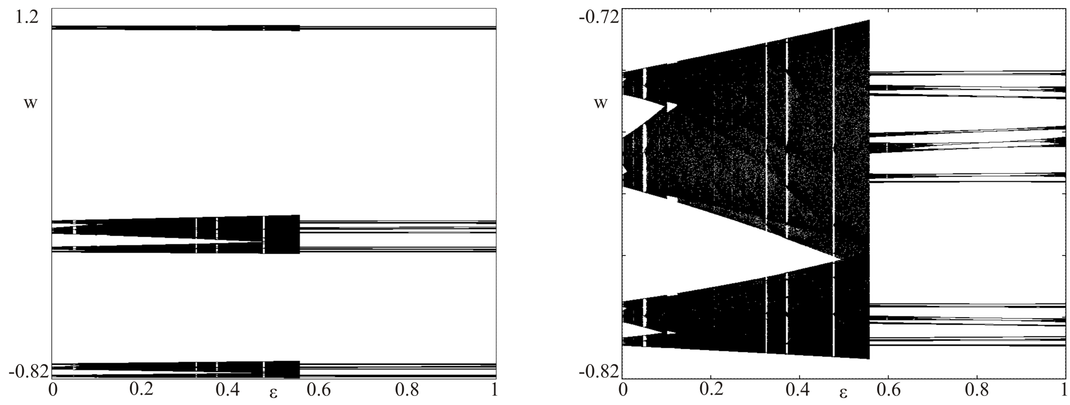

Figure 38. *The bifurcation diagram of variable w versus the coupling strength ε.*

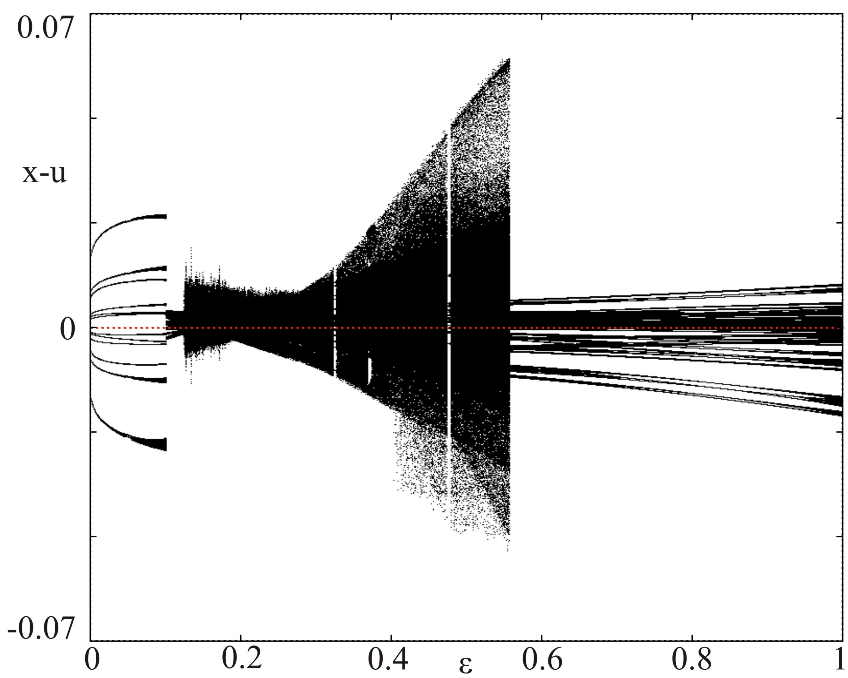

Figure 39. *The diagram of the difference $x - u$ versus the coupling strength ε.*

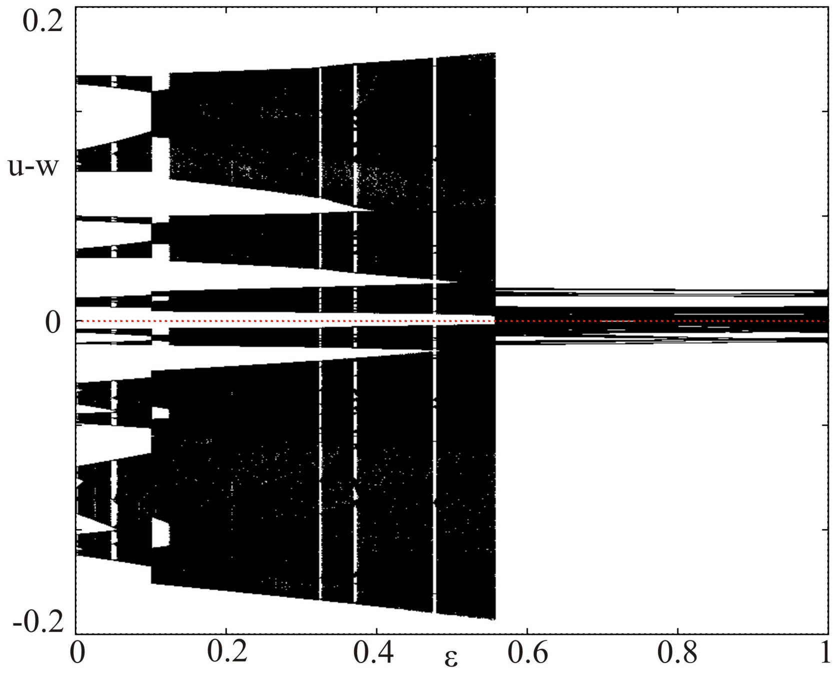

Figure 40. *The diagram of the difference $u - w$ versus the coupling strength ε.*

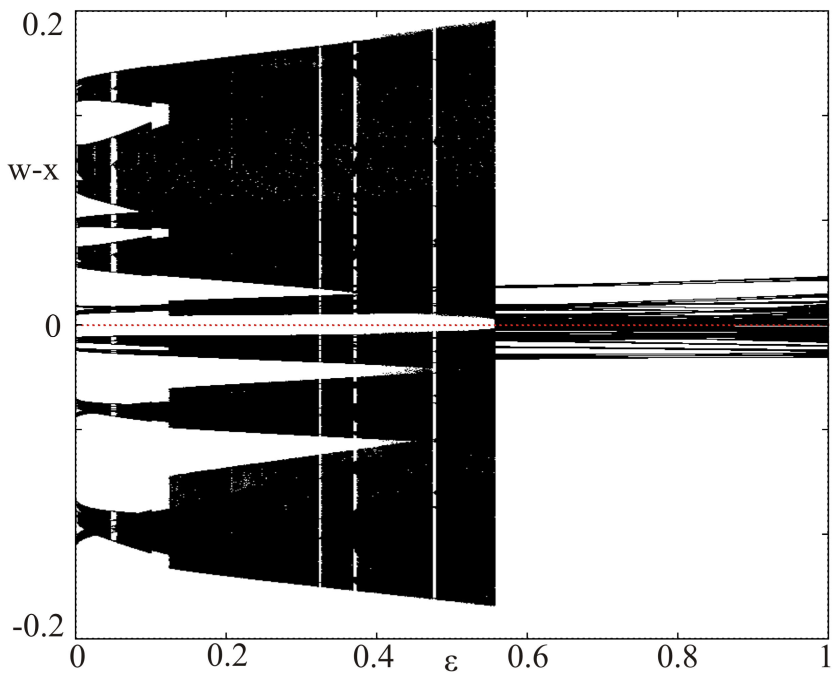

Figure 41. *The diagram of the difference $w - x$ versus the coupling strength ε.*

We may notice that for $\varepsilon \approx 0.558$ *the behaviour of the discussed model changes. For* $\varepsilon \lesssim 0.558$ *maps (4.1) are not synchronized, but for* $\varepsilon \gtrsim 0.558$ *we obtain practical synchronization with* $\delta \leq 0.022$*.* $\delta \leq 0.022$ *may be called small, because it is only approximately 1 percent of the range of* x, u, w *in Figure 36, 37 and 38.*

Let us notice that the rapid decrease of largest Lyapunov exponent to zero indicates synchronization.

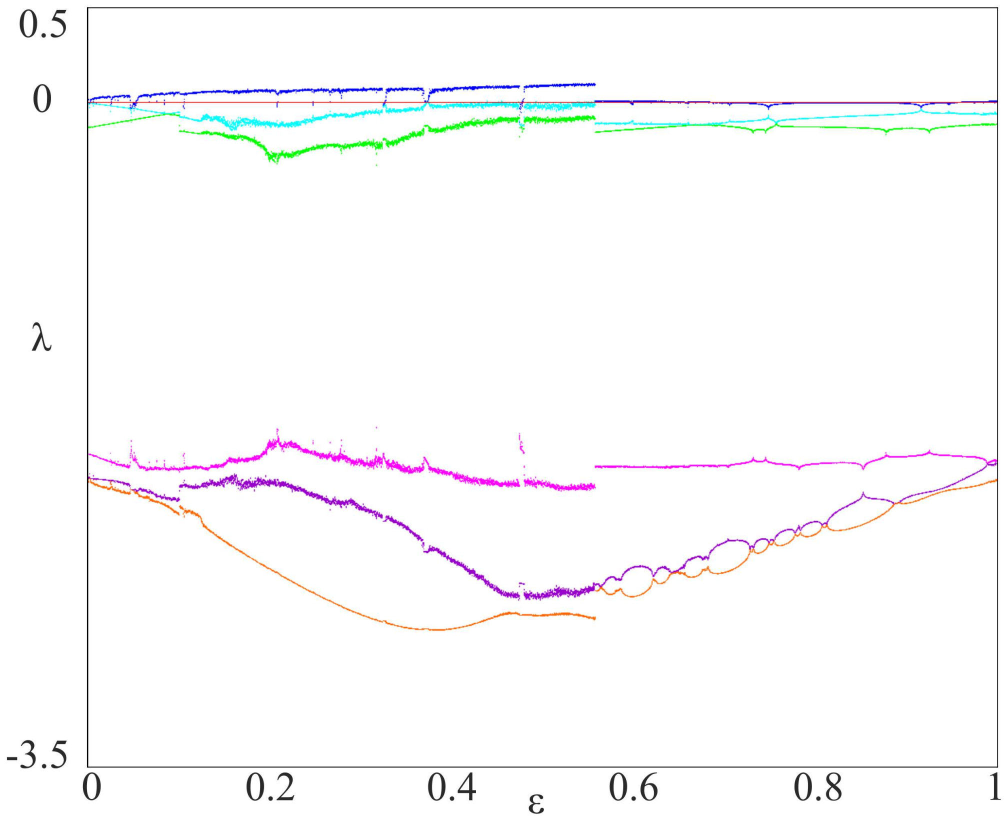

Figure 42. *The Lyapunov exponents versus the coupling strength* ε*. The red line indicate* $\lambda = 0$*.*

According to [1] the points of practically synchronized systems would be situated close to the manifolds $x \equiv u$, $u \equiv w$ *and* $w \equiv u$*. Hence, let us notice in diagrams showing relation between* x *and* u, u *and* w, w *and* x *(Figure 43, 44 and 45) that indeed for* $\varepsilon = 0.55$ *maps are not synchronized and for* $\varepsilon = 0.57$ *they are synchronized.*

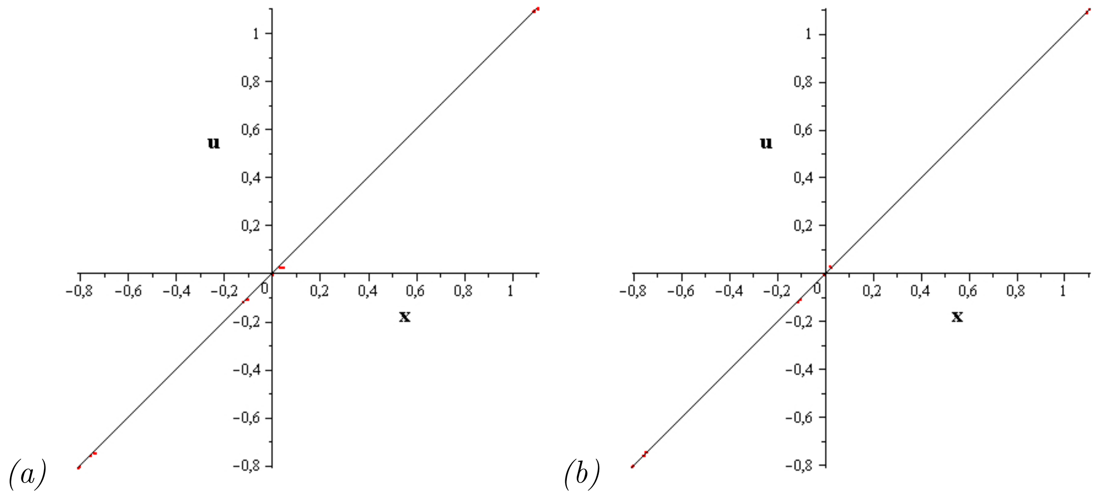

Figure 43. *The projection on the plane* (x,u) *of attractor for (a)* $\varepsilon = 0.55$*, (b)* $\varepsilon = 0.57$.

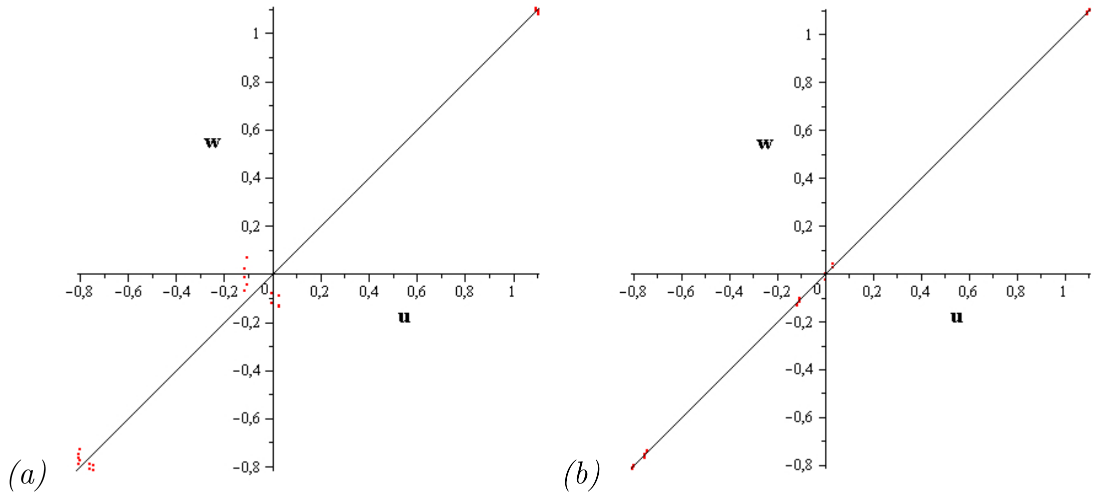

Figure 44. *The projection on the plane* (u,w) *of attractor for (a)* $\varepsilon = 0.55$*, (b)* $\varepsilon = 0.57$.

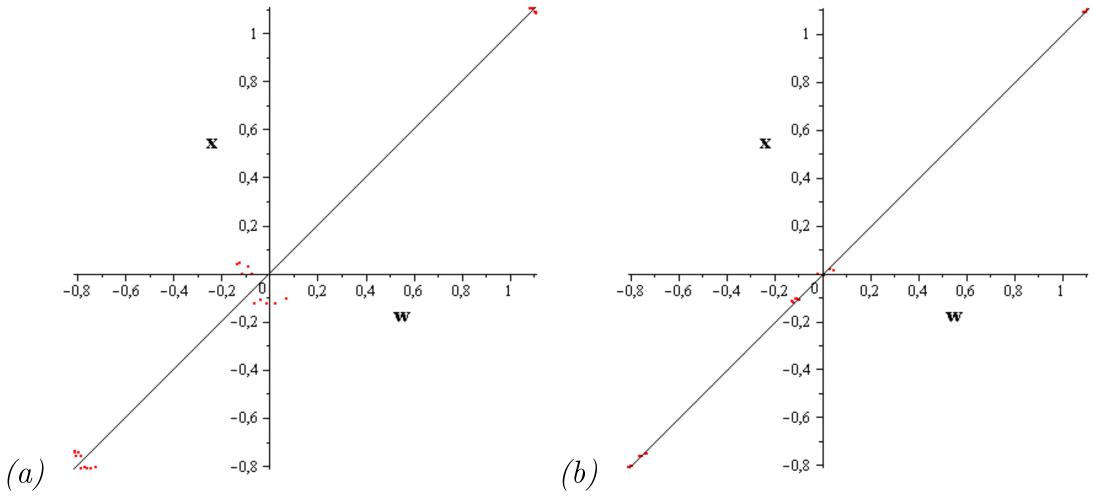

Figure 45. *The projection on the plane (w, x) of attractor for (a) $\varepsilon = 0.55$, (b) $\varepsilon = 0.57$.*

Example 8. *$H_{2,6}$ in period 6, $H_{4,12}$ in period 12, $H_{4,C}$ in chaotic attractor*

Calculating the bifurcation diagrams of Figure 46-48 we start with the following initial conditions for $\varepsilon = 0$: $x_0 = -0.1117857714$, $y_0 = 0.1110876031$, $u_0 = -0.8024975960$, $v_0 = -0.1520331437$, $w_0 = -0.8017949381$ and $z_0 = -0.1518078345$.

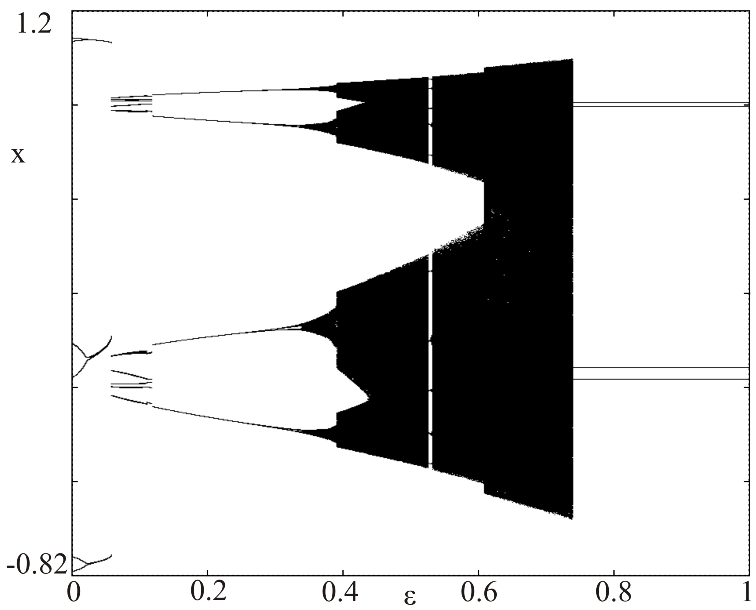

Figure 46. *The bifurcation diagram of variable x versus the coupling strength ε.*

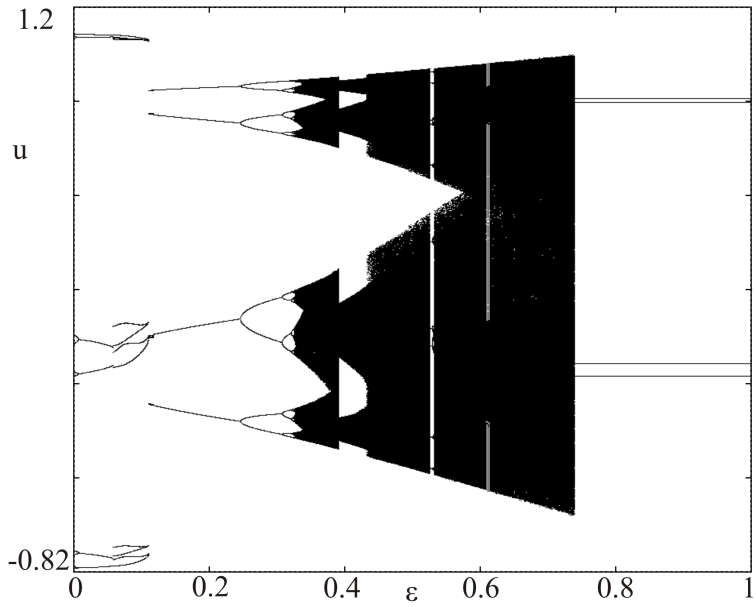

Figure 47. *The bifurcation diagram of variable u versus the coupling strength ε.*

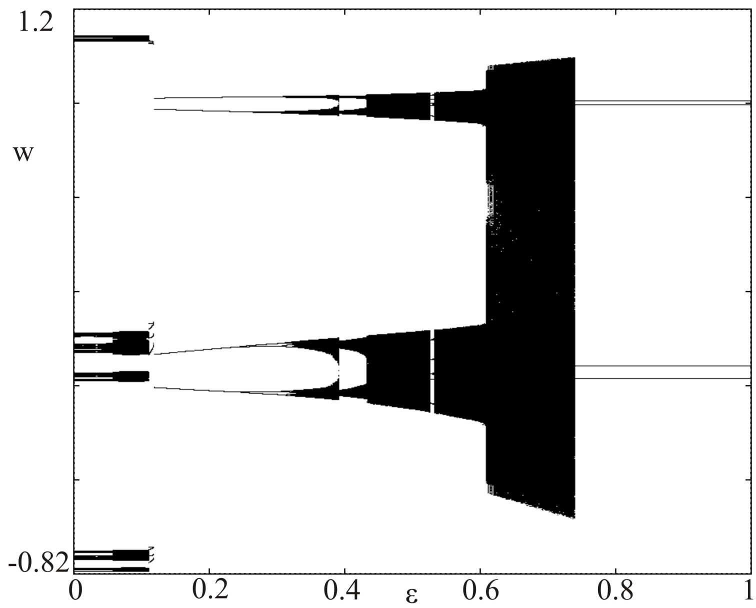

Figure 48. *The bifurcation diagram of variable w versus the coupling strength ε.*

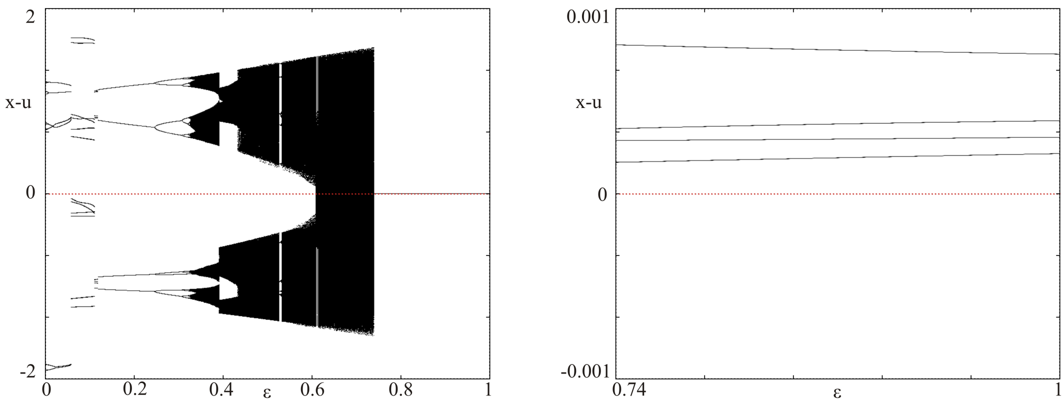

Figure 49. *The diagram of the difference $x - u$ versus the coupling strength ε.*

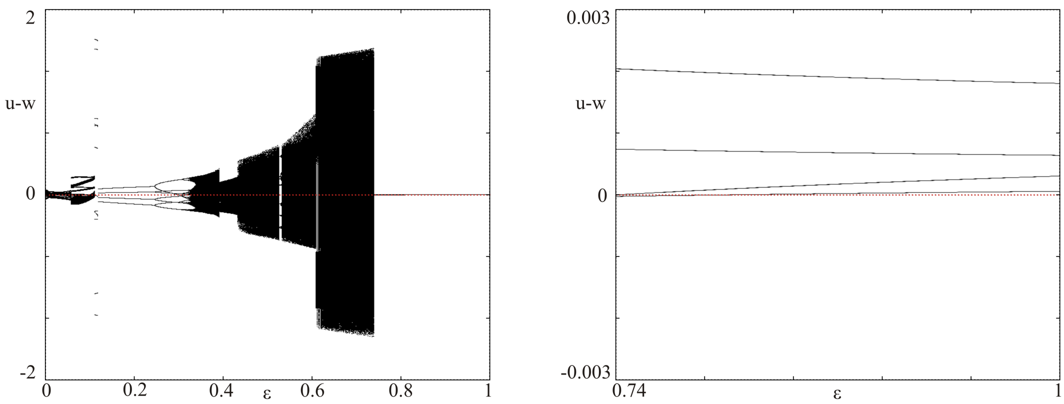

Figure 50. *The diagram of the difference $u - w$ versus the coupling strength ε.*

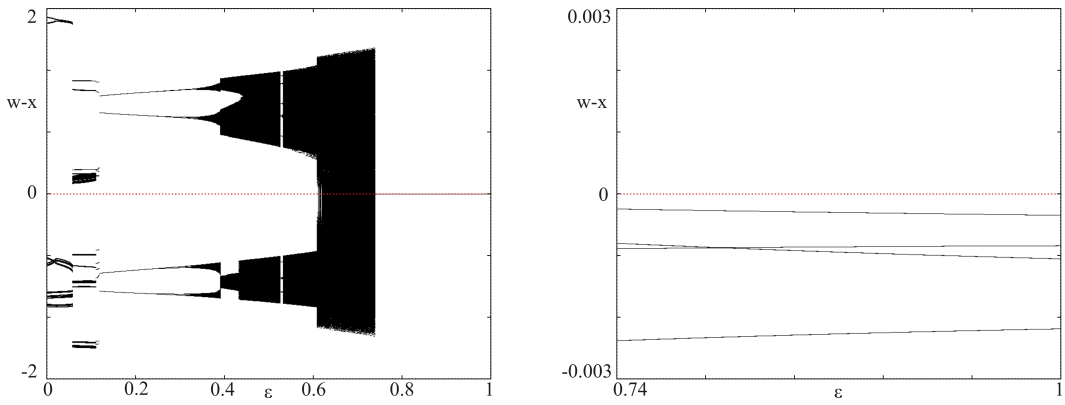

Figure 51. *The diagram of the difference $w - x$ versus the coupling strength ε.*

Analysing Figure 49, 50 and 51 we may find $\varepsilon^* \approx 0.74$ *such that for every* $\varepsilon \in [\varepsilon^*, 1]$ *we obtain very effective practical synchronization with* $\delta \lesssim 0.0024$*. It is also worth noting that for* $\varepsilon \in (0, \varepsilon^*)$ *maps are not synchronized.*

Example 9. $H_{2,6}$ *in period 6,* $H_{4,12}$ *in period 12,* $H_{4,C}$ *in chaotic attractor*

Calculating the bifurcation diagrams of Figure 52-54 we start with the following initial conditions for $\varepsilon = 0$*:* $x_0 = 0.8665180648$*,* $y_0 = 0.01340043371$*,* $u_0 = -0.1064446776$*,* $v_0 = 0.1107446677$*,* $w_0 = -0.7991752643$ *and* $z_0 = -0.1516632986$*.*

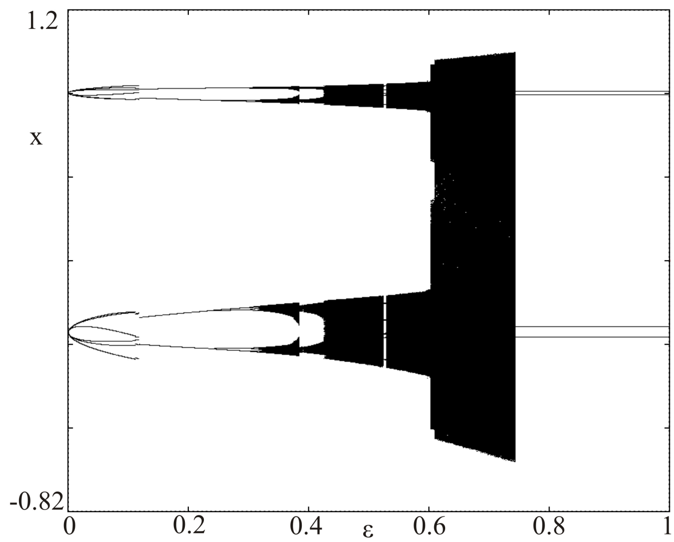

Figure 52. *The bifurcation diagram of variable x versus the coupling strength ε.*

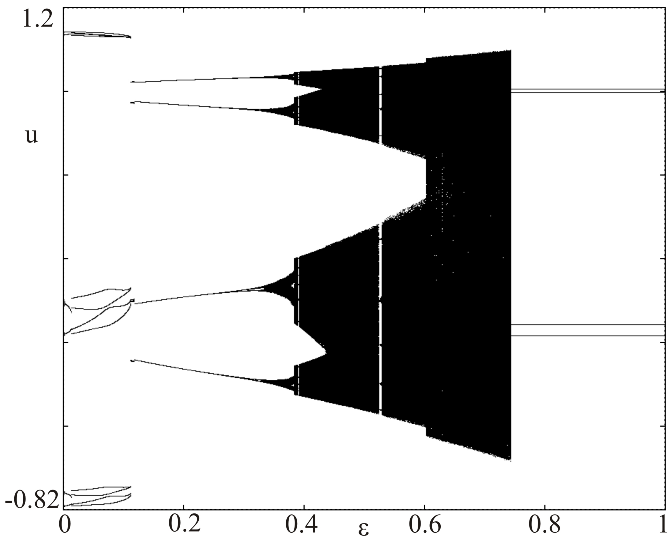

Figure 53. *The bifurcation diagram of variable u versus the coupling strength ε.*

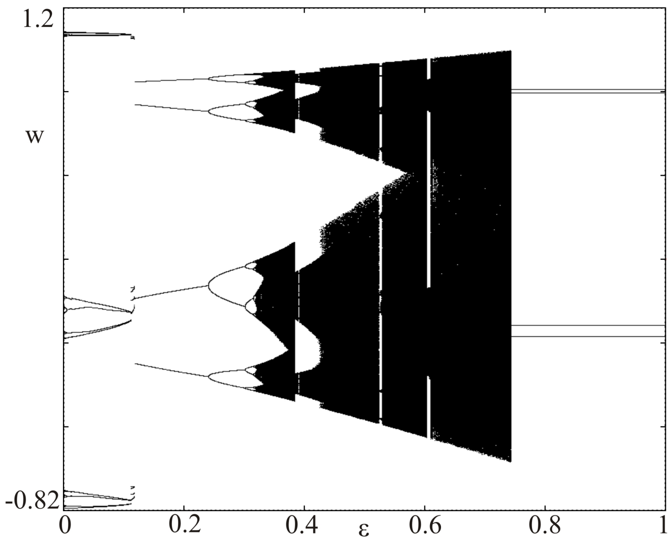

Figure 54. *The bifurcation diagram of variable w versus the coupling strength ε.*

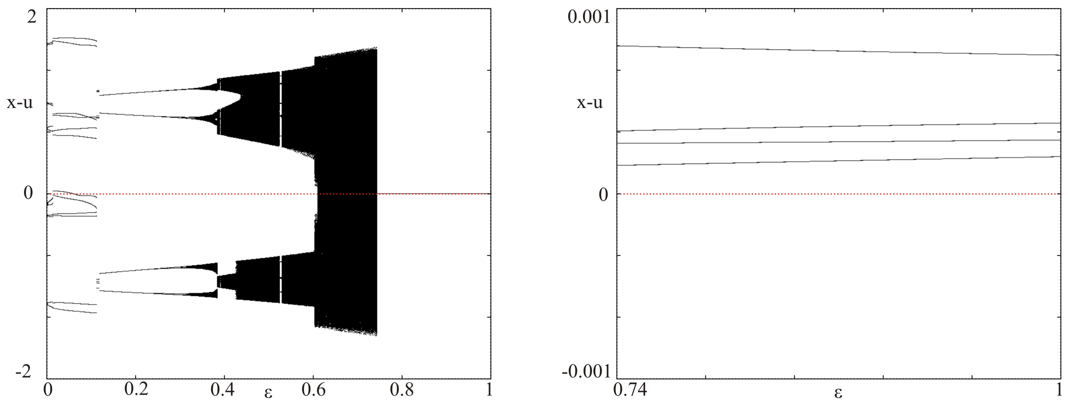

Figure 55. *The diagram of the difference $x - u$ versus the coupling strength ε.*

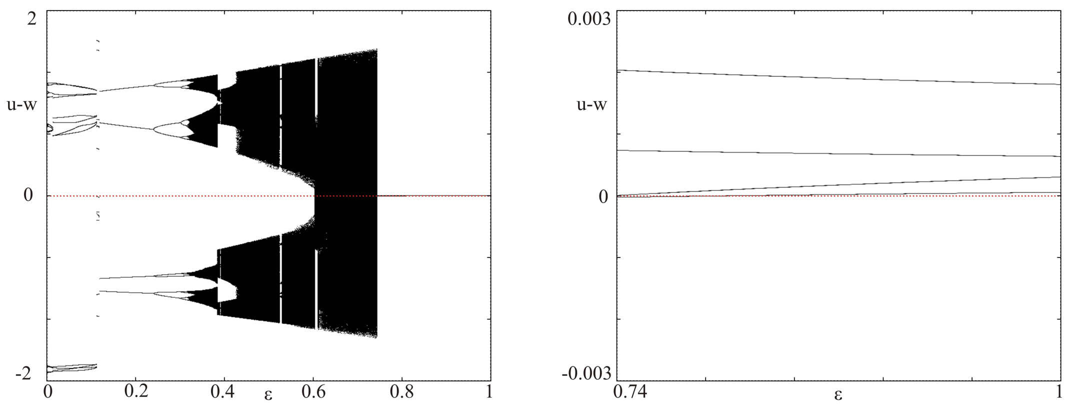

Figure 56. *The diagram of the difference $u - w$ versus the coupling strength ε.*

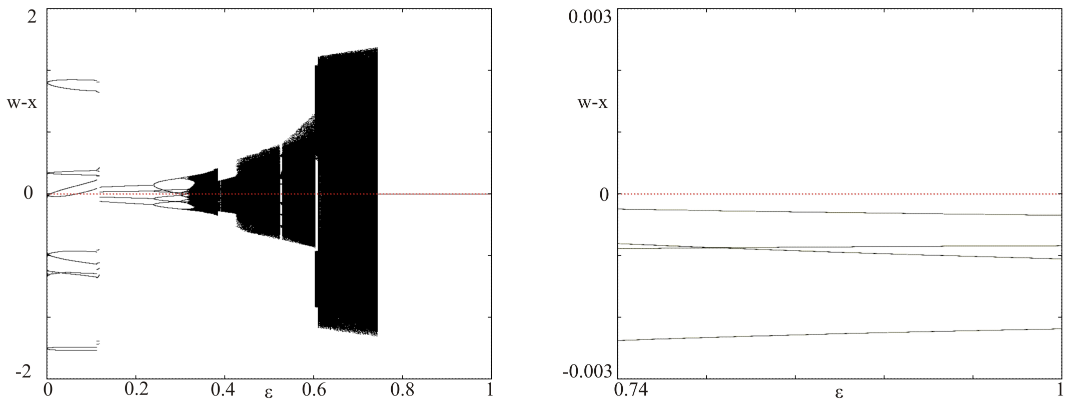

Figure 57. *The diagram of the difference $w - x$ versus the coupling strength ε.*

Analysing Figure 55, 56 and 57 we may find $\varepsilon^* \approx 0.74$ *such that for every* $\varepsilon \in [\varepsilon^*, 1]$ *very effective practical synchronization with* $\delta \lesssim 0.0024$ *is obtained. For* $\varepsilon \in (0, \varepsilon^*)$ *maps are not synchronized.*

It might be observed that in every analysed case for far initial conditions we obtain the same parameter ε^* *and* δ*.*

Example 10. *We will investigate now a different model, which couples three maps previously introduced as* $H_{12,C}$*:*

$$\begin{cases} x_{n+1} = 1 - 1.4847x_n^2 + y_n + \varepsilon(z_n - y_n), \\ y_{n+1} = -0.138x_n, \\ u_{n+1} = 1 - 1.4847u_n^2 + v_n + \varepsilon(y_n - v_n), \\ v_{n+1} = -0.138u_n, \\ w_{n+1} = 1 - 1.4847w_n^2 + z_n + \varepsilon(v_n - z_n), \\ z_{n+1} = -0.138w_n, \end{cases} \tag{4.2}$$

where ε *is the strength of coupling and* $\varepsilon \in [0, 1]$.

Behaviour of the model (4.2) will be examined for initial values in the chaotic attractor, i.e., $x_0 = 1.088483611$, $y_0 = 0.01725281117$, $u_0 = 1.088386849$, $v_0 = 0.01729527084$, $w_0 = 1.088825968$, $z_0 = 0.01710160090$.

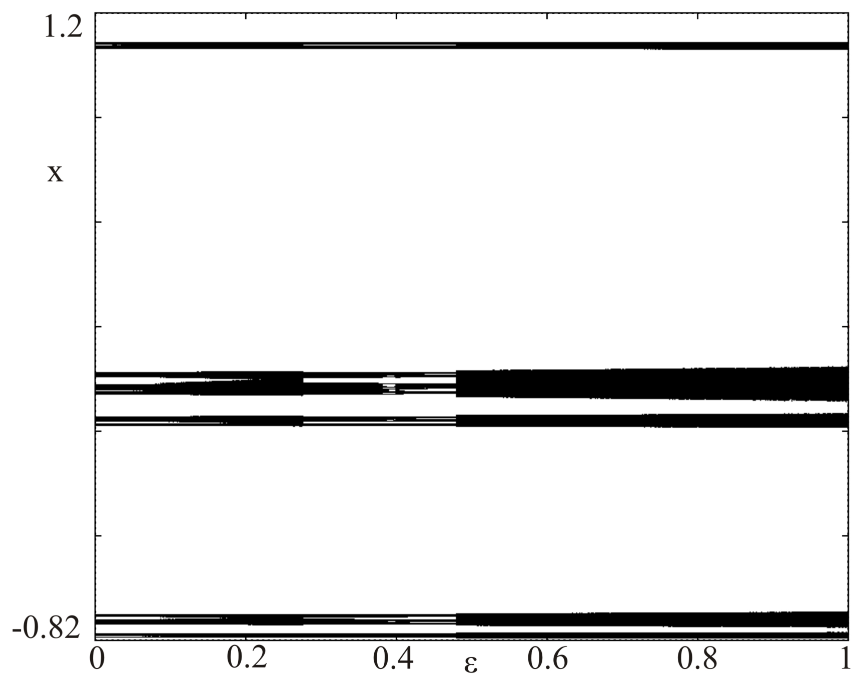

Figure 58. *The bifurcation diagram of variable x versus the coupling strength* ε*.*

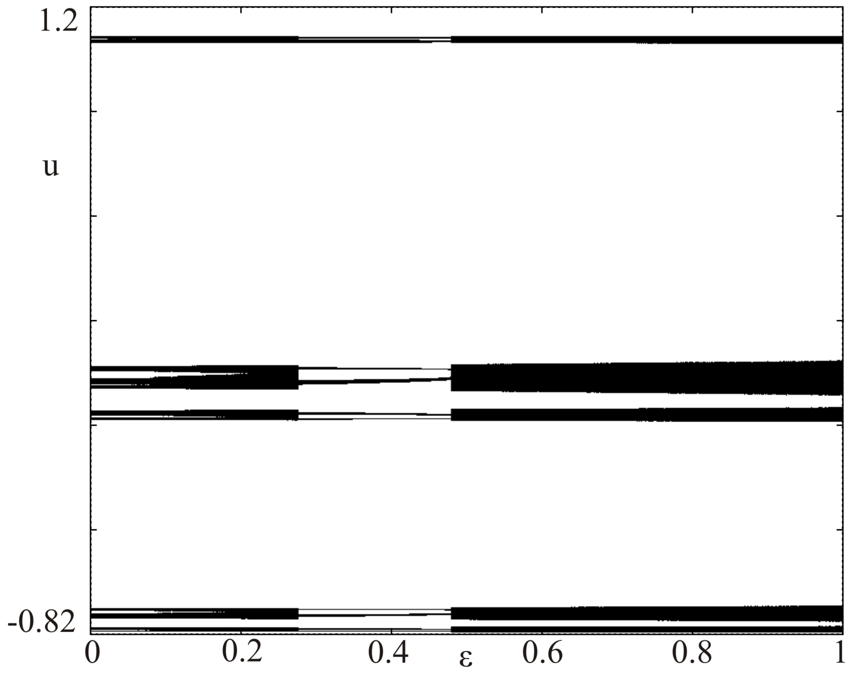

Figure 59. *The bifurcation diagram of variable u versus the coupling strength ε.*

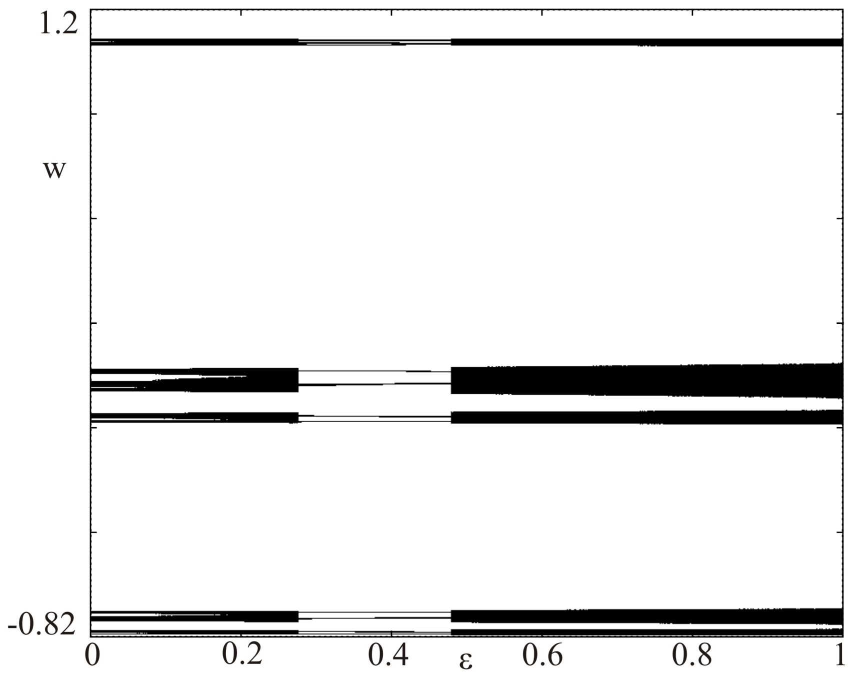

Figure 60. *The bifurcation diagram of variable w versus the coupling strength ε.*

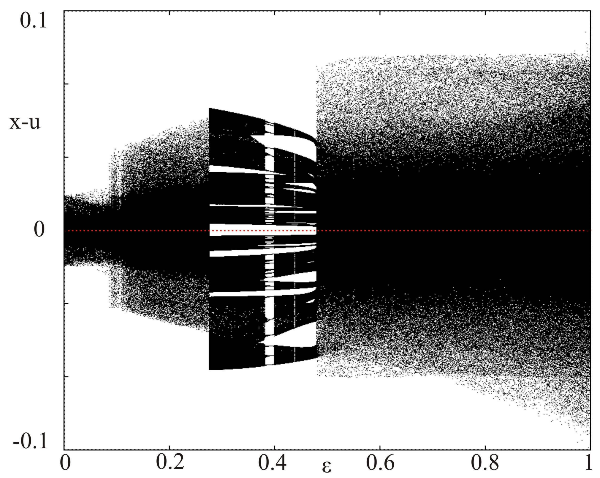

Figure 61. *The diagram of the difference $x - u$ versus the coupling strength ε.*

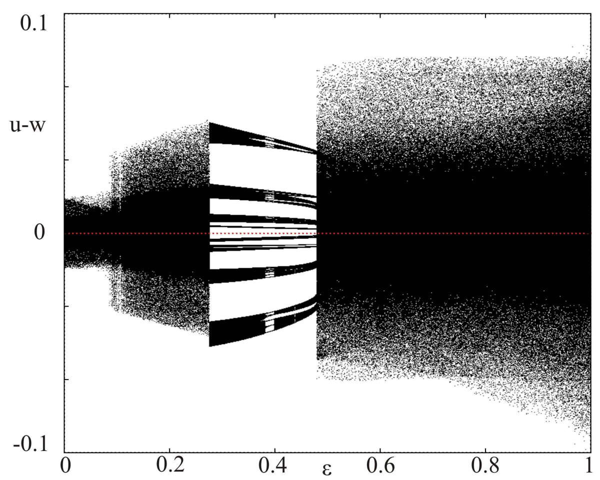

Figure 62. *The diagram of the difference $u - w$ versus the coupling strength ε.*

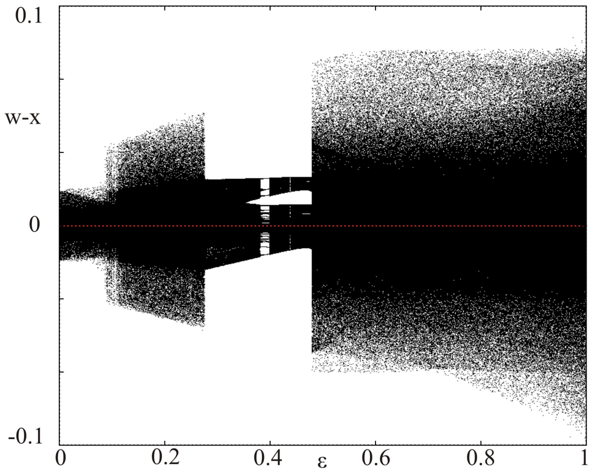

Figure 63. *The diagram of the difference $w-x$ versus the coupling strength ε.*

It may be observed that there occurs practical synchronization with $\delta \leq 0.1$, which may be called small, because $\delta = 0.1$ is approximately 5 percent of the range of x, u, w in Figure 58, 59 and 60.

Behaviour of the model (4.2) changes when positions of initial values on the attractor is different. That is why (4.2) will be examined for initial values in chaotic attractor, but with a different positions on the attractor than in the previously analysed case. Hence we choose: $x_0 = 0.0370157744$, $y_0 = 0.1021088882$, $u_0 = -0.7991752643$, $v_0 = -0.1516632986$, $w_0 = -0.8017949381$, $z_0 = -0.1518078345$.

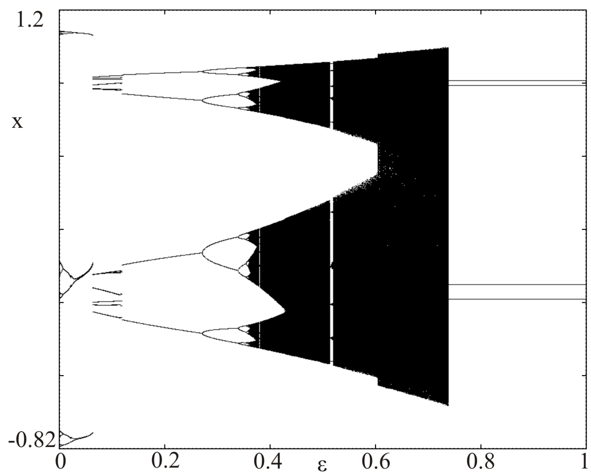

Figure 64. *The bifurcation diagram of variable x versus the coupling strength ε.*

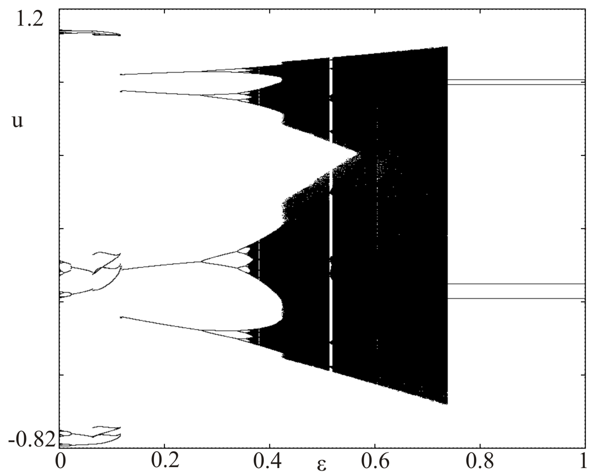

Figure 65. *The bifurcation diagram of variable u versus the coupling strength ε.*

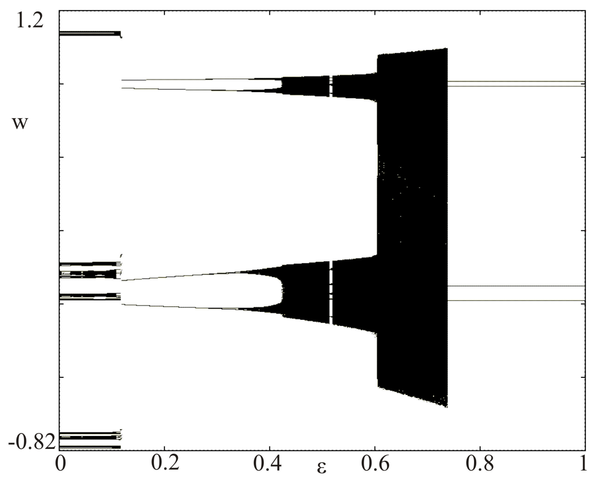

Figure 66. *The bifurcation diagram of variable w versus the coupling strength ε.*

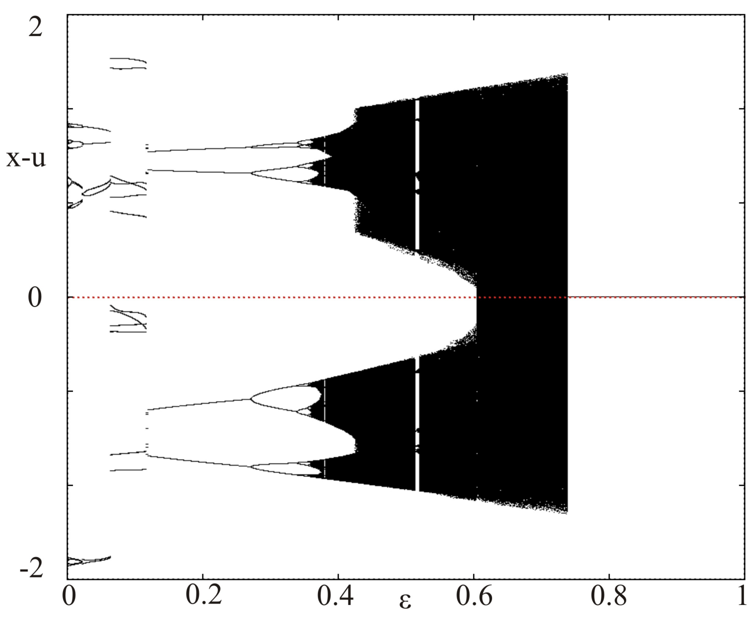

Figure 67. *The diagram of the difference $x - u$ versus the coupling strength ε.*

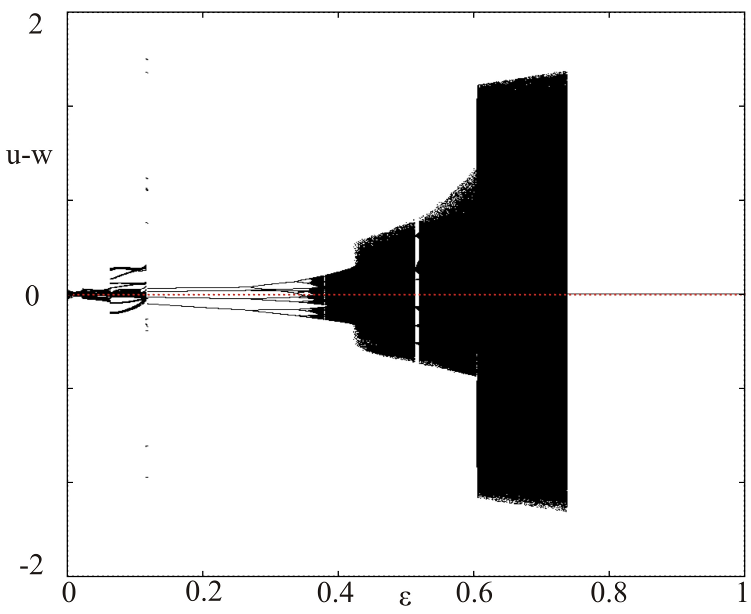

Figure 68. *The diagram of the difference $u - w$ versus the coupling strength ε.*

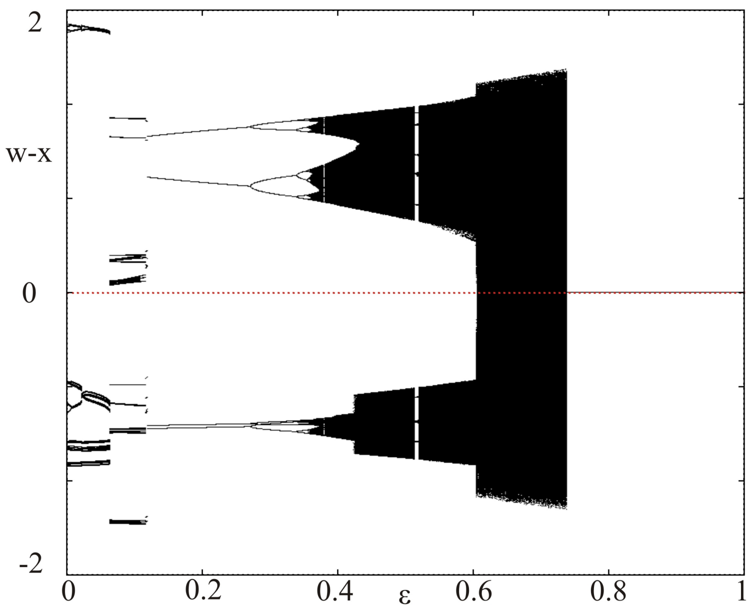

Figure 69. *The diagram of the difference $w - x$ versus the coupling strength ε.*

The evolution of the considered case might be seen also by analysing Lyapunov exponents:

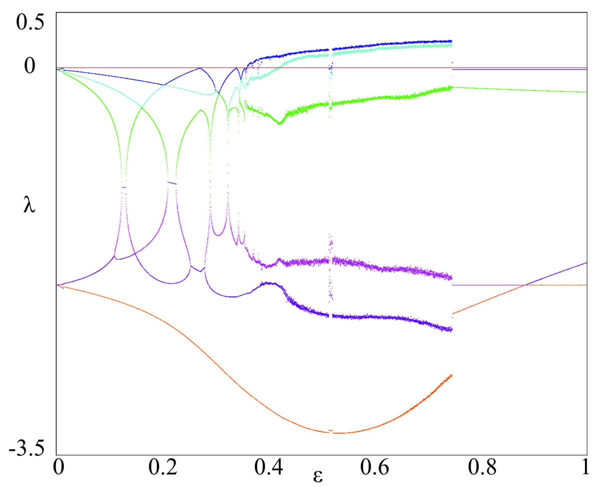

Figure 70. *The Lyapunov exponents versus the coupling strength ε. The red line indicate $\lambda = 0$.*

For $\varepsilon \gtrsim 0.74$ we obtain ideal synchronization. The ideal synchronization is indeed possible here, due to the fact that we have coupled identical maps.

Chapter 5

Conclusions

The Hénon map is a system, which is defined with an easy quadratic equation. Contrary to the possible expectations there are many properties of discussed system, which cannot be proven analytically. That is the reason why in the thesis wide range of numerical analysis was performed. Those numerical analysis show that there are parameters for which the Hénon map is bistable. What is more numerical analyses enabled us to examine different bifurcations and finally the occurrence of the synchronization.

The main conclusion of the performed thesis is the fact that the properties of the coupled maps drastically changes when the position on the attractor for uncoupled system is varied. For $\varepsilon = 0$ coupled maps are iterated till model (4.1) (or (4.2)) is in attractor. That is the reason why synchronization (or its lack) depends on position on attractor in the moment when ε is changed. For each coupling of non-identical maps if the synchronization is obtained, it is always the practical synchronization. For the coupled identical maps the ideal synchronization may be obtained.

Bibliography

[1] Boccaletti S., Kurths J., Osipov G., Valladares D.L., Zhou C.S., *The synchronization of chaotic systems*, Elsevier, 2000.

[2] Sausedo-Solorio J.M., Pisarchik A.N., *Dynamics of unidirectionally coupled bistable Hénon maps*, Elsevier, 2011.

[3] Alligood K.T., Sauer T.D., Yorke J.A., *Chaos - an introduction to dynamical systems*, Springer-Verlag, 1997.

[4] Wiggins S., *Introduction to Applied Nonlinear Dynamical Systems and Chaos*, Springer-Verlag, 2003.

[5] Kuznetsov Y. A., *Elements of Applied Bifurcation Theory*, Springer-Verlag, 1995.

[6] Hénon M., *A Two-dimensional Mapping with a Strange Attractor*, Commun. math. Phys. 50, 69-77, 1976.

[7] Rudnicki R., *Wykłady z analizy matematycznej*, Wydawnictwo Naukowe PWN, 2006.

[8] http://www.mat.ucm.es/ rrportal/numrot1.pdf

[9] Stefański A., Kapitaniak T., *Synchronization of mechanical systems driven by chaotic or random excitation*, Journal of Sound and Vibration, 2003.

[10] Stefański A., *Determining thresholds of complete synchronization, and application*, World Scientific, 2009.